



MID-AMERICA TRANSPORTATION CENTER

Report # MATC-UNL: 227

Final Report



Computational Design Tool for Bridge Hydrodynamic Loading in Inundated Flows of Midwest Rivers

Junke Guo, Ph.D.

Assistant Professor

Department of Civil and Environmental Engineering

University of Nebraska-Lincoln

David M. Admiraal, Ph.D.

Tian C. Zhang, Ph.D.



2010

A Cooperative Research Project sponsored by the
U.S. Department of Transportation Research and
Innovative Technology Administration

The contents of this report reflect the views of the authors, who are responsible for the facts and the accuracy of the information presented herein. This document is disseminated under the sponsorship of the Department of Transportation University Transportation Centers Program, in the interest of information exchange.
The U.S. Government assumes no liability for the contents or use thereof.

MATC

**Computational Design Tool for Bridge Hydrodynamic Loading in Inundated Flows of
Midwest Rivers**

Afzal Bushra, Ph.D.

Graduate Research Assistant

Civil & Environmental Engineering

University of Nebraska-Lincoln

David M. Admiraal, Co-PI

Associate Professor

Civil & Environmental Engineering

University of Nebraska-Lincoln

Tian C. Zhang, Co-PI

Professor

Civil & Environmental Engineering

University of Nebraska-Lincoln

Junke Guo, PI

Assistant Professor

Civil & Environmental Engineering

University of Nebraska-Lincoln

A Report on Research Sponsored By

Mid-America Transportation Center

University of Nebraska-Lincoln

December 2009

Technical Report Documentation Page

1. Report No. 25-1121-0001-227	2. Government Accession No.	3. Recipient's Catalog No.	
4. Title and Subtitle Computational Design Tool for Bridge Hydrodynamic Loading in Inundated Flows of Midwest Rivers		5. Report Date December 2009	
		6. Performing Organization Code	
7. Author(s) Junke Guo, Tian C. Zhang, David M. Admiraal, and Afzal Bushra		8. Performing Organization Report No. 25-1121-0001-227	
9. Performing Organization Name and Address		10. Work Unit No. (TRAIS)	
		11. Contract or Grant No.	
12. Sponsoring Agency Name and Address Mid-America Transportation Center 2200 Vine St. PO Box 830851 Lincoln, NE 68583-0851		13. Type of Report and Period Covered	
		14. Sponsoring Agency Code MATC TRB RiP No. 22332	
15. Supplementary Notes			
16. Abstract <p>The hydraulic forces experienced by an inundated bridge deck have great importance in the design of bridges. The proper estimation of loading exerted by the flow on the structure is important for design plans and is pertinent for evaluating its vulnerability. During a flood or hurricane highway bridges over the sea or other waterways may become partially or completely submerged. Flood flows add significant hydrodynamic loading on bridges, possibly resulting in the shearing or overturning of the bridge deck and failure of the bridge superstructures.</p> <p>The overall objective of the study was to establish validated computational practice to address research needs of transportation community in bridge hydraulics via computational fluid dynamic simulations. The reduced scale experiments conducted at the TFHRC hydraulics laboratory establish the foundations of validated computational practices to address the research needs of the transportation community. The simulations in this study were completed by using the supercomputers at the Argonne National Laboratory. The results of the present research provide a tool for designing new and retrofitting existing bridges so that they are able to withstand the forces and moments that may result from partial or complete inundation.</p>			
17. Key Words		18. Distribution Statement	
19. Security Classif. (of this report)	20. Security Classif. (of this page)	21. No. of Pages 50	22. Price

Table of Contents

LIST OF FIGURES	iv
LIST OF TABLES	vi
ABSTRACT.....	vii
EXECUTIVE SUMMARY	viii
CHAPTER 1 INTRODUCTION	1
CHAPTER 2 LITERATURE REVIEW.....	5
2.1 Hydrodynamic loading on the bridge deck	5
2.2 VOF method	10
CHAPTER 3 METHODOLOGY USED IN SIMULATIONS	13
CHAPTER 4 RESULTS AND ANALYSIS.....	23
4.1 Drag, Lift and Moment coefficients	23
4.2 Contour Plots for Variables Around Scaled Bridge Decks	29
4.2.1 Velocity Contours.....	29
4.2.2 Pressure distribution.....	31
4.2.3 Turbulence kinetic energy.....	36
4.2.4 Turbulence dissipation rate	39
4.2.5 Shear Stress distribution	41
CHAPTER 5 CONCLUSIONS	45
REFERENCES	46
APPENDIX A	49

List of Figures

Figure 1.1 Bridge Hydraulics - US 90 – Biloxi (2005).....	1
Figure 2.1 Force coefficients for the scaled bridge decks.....	7
Figure 3.1 Dimensions of the experimental setup and CFD model scaled 1:1	16
Figure 3.2 Dimension of Prototype Six-girder bridge deck model used in experiments and CFD	17
Figure 3.3 Meshed geometry of six-girder bridge deck model used in CFD (1:1).....	17
Figure 3.4 Dimensions of the experimental setup and CFD model scaled 1:1.5.....	18
Figure 3.5 Dimension of the CFD model scaled by 1:1.5 (smaller).....	19
Figure 3.6 Meshed geometry of bridge deck used in CFD scaled by 1:1.5 (smaller)	19
Figure 3.7 Dimensions of the experimental setup and CFD model scaled 3:1	20
Figure 3.8 Meshed geometry of bridge deck used in CFD scaled by 3:1	21
Figure 3.9 Dimensions of the experimental setup and CFD model scaled 5:1	22
Figure 3.10 Meshed geometry of bridge deck used in CFD scaled by 5:1	22
Figure 4.1 Drag coefficient for Scaled and prototype six-girder bridge deck	25
Figure 4.2 Lift coefficient for Scaled and prototype six-girder bridge deck	26
Figure 4.3 Moment coefficient for Scaled and prototype six-girder bridge deck.....	27
Figure 4.4 (a) Velocity distribution for prototype	30
Figure 4.4 (b) Velocity distribution for 1.5:1 scaled	30
Figure 4.4 (c) Velocity distribution for 1:3 scaled	31
Figure 4.4 (d) Velocity distribution for 1:5 scaled	31
Figure 4.5 (a) Pressure distribution around prototype 1:1 bridge deck	33

Figure 4.5 (b) Pressure distribution for 1.5:1 scaled bridge deck	34
Figure 4.5 (c) Pressure distribution for 1:3 scaled bridge deck	35
Figure 4.5 (d) Pressure distribution for 1:5 scaled bridge deck	36
Figure 4.6 (a) Turbulence kinetic energy distribution around prototype bridge deck	37
Figure 4.6 (b) Turbulence kinetic energy distribution around bridge deck scaled by 1.5:1	38
Figure 4.6 (c) Turbulence kinetic energy distribution for 1:3 scaled bridge deck	38
Figure 4.6 (d) Turbulence kinetic energy distribution for 1:5 scaled bridge deck	39
Figure 4.7 (a) Turbulence dissipation rate around prototype bridge deck	40
Figure 4.7 (b) Turbulence dissipation rate around bridge deck scaled 1.5:1	40
Figure 4.7 (c) Turbulence dissipation rate around bridge deck scaled 1:3	41
Figure 4.7 (d) Turbulence dissipation rate around bridge deck scaled 1:5	41
Figure 4.8 (a) Shear stress distribution on bridge deck for prototype	42
Figure 4.8 (b) Shear stress distribution on bridge deck scaled by 1.5:1	43
Figure 4.8 (c) Shear stress distribution on bridge deck scaled by 1:3	43
Figure 4.8 (d) Shear stress distribution on bridge deck scaled by 1:5	44

List of Tables

Table 4.1 CFD results of drag, lift and moment coefficient for scaled bridge	28
--	----

Abstract

The hydraulic forces experienced by an inundated bridge deck have great importance in the design of bridges. The proper estimation of loading exerted by the flow on the structure is important for design plans and is pertinent for evaluating its vulnerability. During a flood or hurricane highway bridges over the sea or other waterways may become partially or completely submerged. Flood flows add significant hydrodynamic loading on bridges, possibly resulting in the shearing or overturning of the bridge deck and failure of the bridge superstructures.

The overall objective of the study was to establish validated computational practice to address research needs of transportation community in bridge hydraulics via computational fluid dynamic simulations. The reduced scale experiments conducted at the TFHRC hydraulics laboratory establish the foundations of validated computational practices to address the research needs of the transportation community. The simulations in this study were completed by using the supercomputers at the Argonne National Laboratory. The results of the study showed that the critical values of the drag coefficient occur when the bridge is well inundated, but the critical values of the lift and moment coefficients occur near the transition from partially to fully inundated. The critical lift coefficient is negative, which corresponds to a pull-down force.

The CFD results match the experimental data in terms of the relationship between the inundation ratio and force measured at the bridge. The CFD methodology is used to transfer the recent supercomputer models of bridge inundation flows from laboratory scales to small scale and large scales and analyze the effect of scaling on turbulent flow and hydrodynamic forces obtained based on the Froude number similarity method. The results of the present research provide a tool for designing new and retrofitting existing bridges so that they are able to withstand the forces and moments that may result from partial or complete inundation.

Executive Summary

Bridges are typically designed to withstand the 75-year or 100-year flood, but climate change has potential to influence precipitation patterns and storm frequency, resulting in an increased frequency of design storms in many locations. The DOT Center of Climate Change and Environmental Forecasting predicts that as global temperature increases, weather patterns will change (Pottel et al. 2008). For example, two 500-year floods occurred in 1993 and 2008, separately, in the Midwestern United States and states affected by the storms included Illinois, Indiana, Iowa, Michigan, Minnesota, Missouri, and Wisconsin. The latter flood resulted in a Union Pacific bridge failure by high floodwaters on the Cedar River in Iowa on June 10, 2008. These weather changes reduced the return period of design floods of existing bridges, leading to a more frequent inundation of bridge decks.

These events have demonstrated that when bridges are submerged, failure can be costly if not catastrophic. The results of the present research provide a tool for designing new bridges and retrofitting old ones so that they are able to withstand the forces and moments that may result from partial or complete inundation. To consider the potential impacts of climate, a combined experimental and computational study on inundated bridge hydrodynamics was conducted recently. This study was a collaborative effort by FHWA Hydraulics Laboratory, the Argonne National Laboratory, and the University of Nebraska-Lincoln. The study showed that drag, lift and moments on inundated bridge decks in laboratory settings can be accurately predicted using commercially available CFD software, FLUENT and STAR-CD with either a $k-\varepsilon$ model or a Large Eddy Simulation model. This study emphasizes the effect of scaling on turbulent flow and hydrodynamic forces obtained based on Froude similarity method, and extends the method to practical scales.

Physical modeling based on similitude theory is commonly used in research of turbulent flow around the bridge decks. Due to the difficulties of meeting both Froude number and Reynolds number similarities, the small-scale laboratory experiments ignore the effects of Reynolds number and turbulence. Although Froude number similarity generally plays a more important role in gravity driven water flow, effects of turbulence may not be negligible for flows near bridge decks. In this study, numerical simulations were conducted to examine the errors in applying Froude similitude in physical modeling.

In the present CFD study, a six-girder bridge deck model (1:1) was initially validated with the experimental data. The methodology was then used to predict the effect of scaling by using a six-girder bridge deck model scaled to a factor of 1:1.5, 1:1, 3:1 and 5:1. The computed values of drag, lift and moment coefficient for the scaled bridge deck were compared with the simulation results obtained from the experiments (for 1:1 scaled bridge deck). After validating the CFD results (for a 1:1 scaled bridge deck model) with experiment results, a small sized bridge deck, 1:1.5, was simulated and the results were compared. Later, two large sized bridge decks, 3:1 and 5:1, were used to analyze the effect of scaling. The drag coefficients for large and small sized bridges did not show any effect of scaling for drag coefficient at a higher inundation ratio and was found to be approximately 2.2. Nevertheless, at a lower inundation ratio (i.e., $h^* \leq 1.5$) the simulated drag coefficients are about 7%-10% less than the measured data. The lift coefficient showed an overall difference of around 15% in the large and small size bridge deck. This disparity may be due to the difficulties in meeting both Froude number similarity and Reynolds number similarity in which the Reynolds number similarity was neglected and, consequently, the model is distorted. The moment coefficient did not show any effect of scale for the complete range of the inundation ratio. Ignoring the Reynolds number similarity in the

modeling approach therefore did not show any significant effect on the non-dimensional moment coefficient and drag coefficient at higher inundation ratios. However, some effect of scale was observed in lift coefficient and drag coefficient only at the lower inundation ratio. With the limit of the current computational speed, a practical design scale bridge (scale 40:1) could not be created easily because of the significant computational time. For practical design, it is recommended that a small-scale simulation is conducted, and then the results be scaled to a practical case by using the Froude number similarity.

Chapter 1 Introduction

Bridges provide a critical component of the nation's transportation network. Evaluation of bridge stability and structural response after flooding events is critical to highway safety. During a big flood or tsunami, a highway bridge above the sea or waterway may be submerged partially or completely. Such flows add significant hydrodynamic loading on bridges, possibly resulting in the turnover of the bridge decks and failure of the bridge superstructures. Figure 1.1 shows that the 1.6 mile Biloxi-Ocean Springs Bridge, which carries four lanes of US90 between two cities over Biloxi Bay, suffered complete damage during Hurricane Katrina.

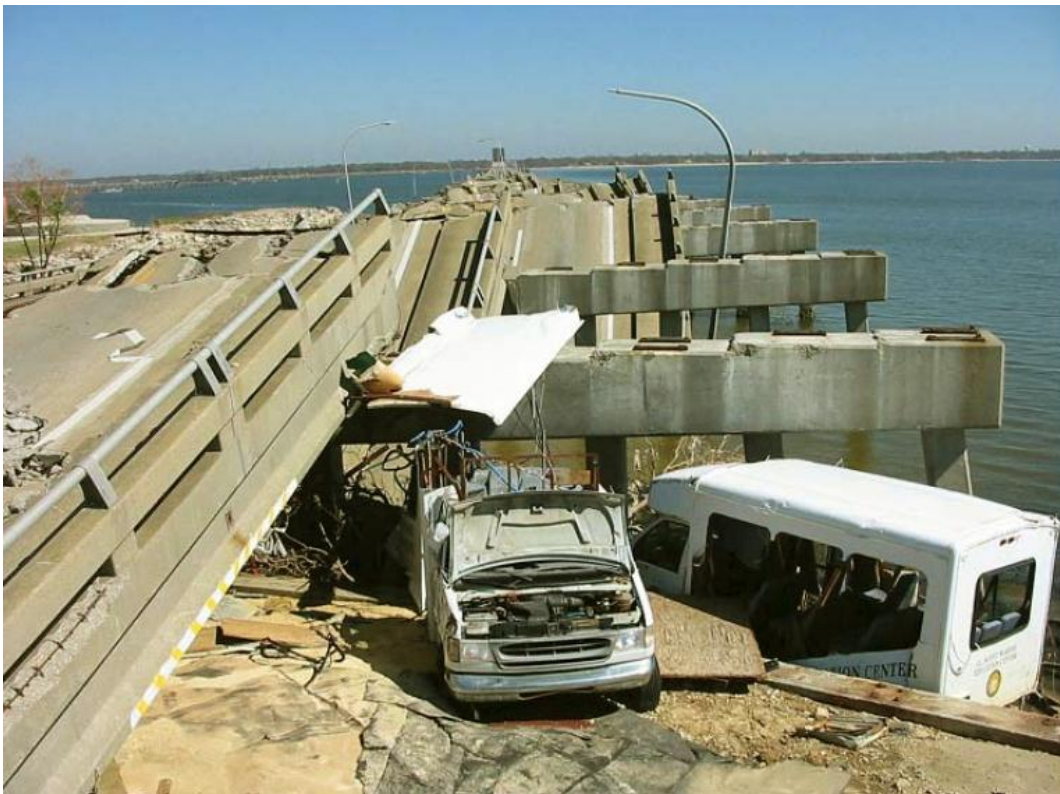


Figure 1.1 Bridge Hydraulics - US 90 – Biloxi (2005)

So far, these events have relied on scaled experiments to provide measurements for flow field structural response with expensive cost. With rapid development of supercomputing

technology, commercial Computational Fluid Dynamics (CFD) code provides a quick, economic way to study these systems. The availability of parallel computers and analysis capabilities of commercially available software provide an opportunity to shift the focus of these evaluations to CFD domain. When validated using the broad experimental database, the use of CFD simulations allow expanded parametric analysis and provide a means of evaluating directly the effects of scaling. Therefore, in the present study, the Computational Fluid Dynamics (CFD) technique is used for simulating open channel flow around inundated bridges. The reduced scale experiments conducted at TFHRC (FHWA) hydraulics laboratory are used to validate the simulation results.

CFD provides a qualitative prediction of fluid flow by means of numerical modeling and software tools. It enables scientists and engineers to perform experiments (i.e., computer simulations) in a virtual flow laboratory and significantly reduces the amount of experimentation and the overall cost. CFD is a highly interdisciplinary research area that lies at the interface of physics, applied mathematics and computer science. The CFD simulations in this study focus on the applicability of the commercial CFD software, FLUENT, for prediction of flow field, drag and lift forces on flooded bridge decks with different deck shapes.

Bridges are typically designed to withstand the 75-year or 100-year flood, but climate change has potential to influence precipitation patterns and storm frequency, which increases frequency of design storms in many locations. The DOT Center of Climate Change and Environmental Forecasting predicted that as global temperature increases, weather patterns would change (Pottel et al. 2008). For example, two 500-year floods occurred in 1993 and 2008, separately, in the Midwest United States (including Illinois, Indiana, Iowa, Michigan, Minnesota, Missouri, and Wisconsin) which resulted in a Union Pacific bridge failure by high floodwaters

on the Cedar River, Iowa on June 10, 2008. These weather changes reduced the return period of design floods of existing bridges, leading to a more frequent inundation of affected bridge decks. These events have demonstrated that when bridges are inundated failure can be costly, if not catastrophic. The results of the present research provide a tool for designing new bridges and retrofitting existing ones so that they are able to withstand the forces and moments that may result from partial or complete inundation. To consider the potential impacts of climate a combined experimental and computational study on inundated bridge hydrodynamics was conducted in a collaborative effort by the FHWA Hydraulics Laboratory, the Argonne National Laboratory, and the University of Nebraska-Lincoln. This study showed that drag, lift and moments on inundated bridge decks in laboratory settings can be accurately predicted using commercially available CFD software, FLUENT or STAR-CD with either a $k-\varepsilon$ model or a Large Eddy Simulation model. The present study analyzes the effect of scaling on turbulent flow and hydrodynamic forces obtained from Froude similarity method, and then transfers the recent supercomputer models of bridge inundation flows from laboratory scales to practical scales.

Physical modeling based on similitude theory is commonly used in research of turbulent flow around the bridge decks. Due to the difficulties of meeting both Froude and Reynolds similarities, the small-scale laboratory experiments ignore the effects of Reynolds number and turbulence scale. Although Froude similarity generally perform a more important role in gravity surface water flow, effects of large turbulence scale may not be negligible for flows near bridge decks. In this study, numerical simulations were conducted to examine errors when applying Froude similitude in physical modeling.

Effects of scaling on the bridge decks due turbulent flow and hydrodynamic forces are studied using the computational fluid dynamic simulations of the three-dimensional model. The

methodology used to predict the non-dimensional hydrodynamic forces of bridge inundation flows was transferred from laboratory scales to the small- and large-scale models. A small size bridge deck scaled to a factor of 1:1.5 than the one used in experiments was used initially to predict the effect of scaling. After validating the results of the small-scale bridge with those obtained from laboratory scales, a six-girder bridge deck scaled to a factor of 3:1 and 5:1 bigger than the one used in the laboratory was investigated. The drag, lift and moment coefficients acting on the scaled bridge deck were numerically calculated for the scaled model that was based on the geometrical similarity and Froude number similarity laws. Nevertheless, the model was distorted because it did not meet the requirements of the Reynolds number similarity. Effects of scaling on hydrodynamic forces are being investigated by comparing the results obtained from the experiments and the scaled numerical model. Since the practical design would be 40 times bigger than the experimental model and computationally intensive—requiring a huge amount of computational time—only two large scaled bridges are used, scaled to a factor of 3:1 and 5:1.

Chapter 2 Literature Review

Highway bridges, as the important infrastructure of transportation, are especially vulnerable to the landfall of hurricanes that result in extreme storm surges. During hurricanes waves are capable of affecting and inundating the bridge deck, or even damaging the whole bridge superstructure. Therefore, many state departments of transportation have already deployed related research topics, including the vulnerability of bridges and the design of bridge decks or piers, in order to minimize the effect of waves or a storm surge.

Many researchers have conducted experiments to predict the non-dimensional hydrodynamic forces acting on inundated bridge decks, discussed in further detail in the next section. This literature review consists of two sections: the non-dimensional hydrodynamic forces on the bridge deck, and the Volume of Fluid (VOF) methodology used by the previous researchers.

2.1 Hydrodynamic loading on the bridge deck

The Federal Highway Administration (FHWA) research on the hydrodynamic loads on piers and the bridge deck has provided some estimates of wave loads acted on the damaged bridge deck. The results of the study showed that the combined mechanisms of wave-induced loads from free surface alteration and buoyancy loads are the major causes for the failure of bridge decks or superstructure (Douglass 2006). Wave-induced loads from the free surface and buoyancy loads from the internal flow have a significant influence of drag, lift and moment acted on the bridge decks, which leads to the damage or turnover of bridge superstructure.

Tainsh (1965) performed experiments for the three and four girder bridge deck, and for totally submerged and partially submerged bridges. The bridge deck was adjusted to the proper elevation in order to ignore the influence of the channel floor. Force loads on the bridge were

evaluated by measuring the pressure distribution on girders, however the contribution of the shear stresses along the bridge deck surface was not considered in this study.

Denson (1982) measured the hydrodynamic forces for three types of bridge decks with girders for various inundation ratios. Denson studied the dependence of the force coefficients on a bridge Froude number, V/\sqrt{gl} , relative inundation depth, h/l , and relative thickness of the bridge, s/l . Here, h is the inundation depth (or the water depth upstream the bridge), l is the total bridge length in the flow direction, V is the upstream mean flow velocity, g is gravity, and s is the total bridge thickness. The drag and lift coefficients were evaluated using the parameters s and l , respectively, as characteristic length, l^2 , was used for analyzing the momentum coefficient. Although an extensive series of data were presented, no interpretation of the physical meaning of the evidenced dependencies was offered by this study. Both Tainsh (1965) and Denson (1982) assumed the parameters to be independent of the Reynolds number.

Naudascher and Medlarz (1983) used the dynamometer to obtain directly the drag acting on the bridge girders. They observed that flow moving past bridge girders is unstable and gives rise to a, more or less, periodic vortex formation and fluctuation of the dynamic force acting on the bridge. They also analyzed the effects of the elevation of the bridge and the angle between the flow and the bridge axis on time-averaged hydrodynamic loads for a partially submerged bridge. They also introduced a relationship between the drag coefficient and the controlling parameters.

Okajima et. al (1997) analyzed the blockage effect on the drag coefficient for a rectangular bridge deck. The results showed that drag coefficient increases with an increasing

blockage ratio (s/h , where s is the thickness of the cylinder and h is the depth of the upstream flow).

Matsuda et al. (2001) analyzed the effects of scaling on drag, lift and moment coefficient for bridge deck models with different scales. Three sizes of bridge deck models were analyzed: including a 1:10 scale model, 1:30 scale model and 1:80. The drag coefficient, lift coefficient and moment coefficient were studied for varying angles of attack for three different scales of bridge deck in a wind tunnel. The drag, lift and moment coefficient showed a variation for various angles of attack. However, for a particular angle of attack, the scaled bridges did not show any variation in C_D , C_L and C_M (Fig. 2.1), showing that C_D , C_L and C_M is independent of the scale of the model.

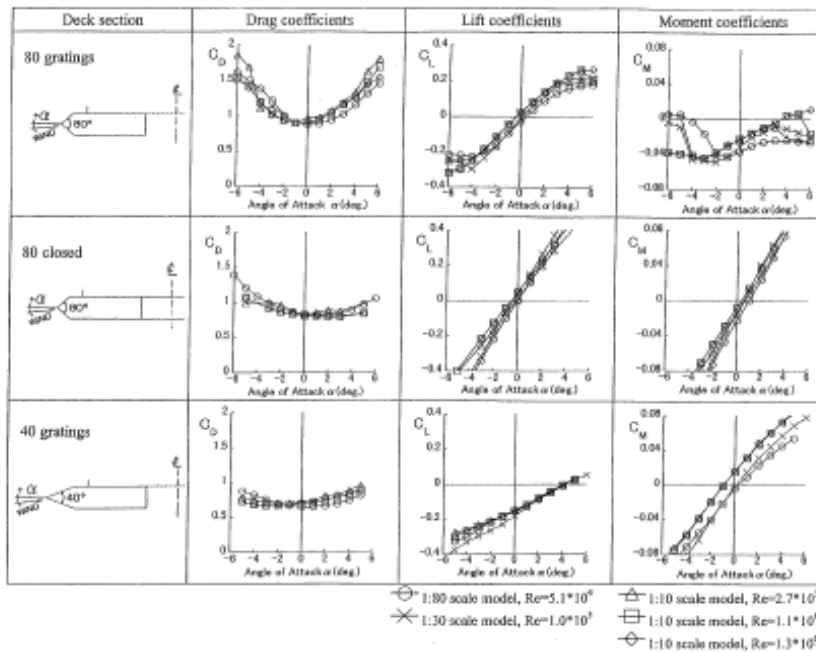


Figure 2.1 Force Coefficients for the Scaled Bridge Decks (Matsuda Et Al, 2001)

Malavasi and Guadagnini (2003) performed laboratory experiments to quantify the hydrodynamic loading on a bridge deck with a rectangular cross section. The measurements were made for time-varying hydrodynamic forces acting on the obstacle for various inundation ratios and deck Froude number. They analyzed the experimental results via dimensional analysis and relationships between time-averaged force coefficients (drag, lift, and moment coefficients), the deck Froude number and geometrical parameters. Their results showed that due to the presence of a free surface, force coefficients can either be larger (by more than a factor of 2) or lower than the corresponding values of an unbounded domain.

Malavasi and Guadagnini (2003) compared the drag and lift coefficient for a bridge deck modeled as a cylinder of rectangular cross section with those having girders. The bridge deck with girders and those with a rectangle showed reasonable overall comparability. In the case of the rectangular cross section, the difference was observed in the sharp peak at $h^* = 1.2$ for drag coefficient; the difference may be a consequence of the difference in shape. The girder bridge model had solid guardrails above the deck and girders below, and the shear layers separating from the upper- and lower-edges of these were placed at large distances from the deck. In the case of rectangular sections, the shear layers separated from the corners of the deck and the sharp peaks for drag coefficient may be caused by interactions between these layers and the deck downstream.

Malavasi et al. (2004) investigated the flow field around a submerged bridge deck. The deck submersion was found to be a critical situation for the structural stability of river bridges. This study characterized the large-scale vortexes in the bridge wake by using the PIV technique. The bridge was modeled as a rectangular cylinder. The flow fields around the deck had shown strong asymmetry and a complex vortex-shedding regime.

Cigada et al. (2001) developed a measurement system to characterize the hydrodynamic forces due to the interaction between a free surface flow and a bridge deck. The bridge deck was modeled as a rigid box and placed in a laboratory flume to study the interaction with the flow by measuring the force exchanged between the current and the deck. They analyzed two possible solutions to evaluate the dynamic forces exchanged between the flow and the bridge: distributed pressure taps and direct force measurements.

In environmental hydraulics the drag, lift and moment coefficients on objects under specified flow condition have been extensively studied. Although the definition of the drag, lift and moment and theoretical derivation are clear, the specific formula is almost impossible based on the theoretical derivation due to the force coefficients' dependence on the shape of objects. Generally, the approach of dimensional analysis combined with the physical experiments is used to evaluate the relationship between the force coefficients and other variables: such as the geometry of obstruction, Reynolds Number, and the bridge opening. All of the previous work on the hydrodynamic forces acting on an obstacle has been conducted using experiments or dimensional analysis. The bridge analysts and designers have relied on expensive scaled experiments to provide estimates of the flow field and structural response. With the rapid development of supercomputing technology, commercial CFD code provides a quick, economic way to study these systems. The availability of parallel computers and analysis capabilities of commercially available software provides an opportunity to shift these evaluations into the CFD domain. The use of CFD simulations will allow expanded parametric analysis and provide a means of directly evaluating the effects of scaling.

2.2 VOF method

Many researchers conducted their own experiments for open channel turbulent flow and simulated experimental testing to compare simulation outcomes with experimental results. With successful use of Volume of Fluid (VOF) methodology, they found good agreement between simulation and experimental results.

Harlow and Welch (1965) developed a new technique called the marker and cell method for numerical calculation of transient viscous incompressible flow with free surface. Navier-Stokes equations were written in finite difference form, and finite time step advancement was used to calculate solutions. It was found that this technique is successfully applicable to a wide variety of two- and three-dimensional applications for free surface.

Koshizuka, Tamako and Oka (1995) presented a particle method for transient incompressible viscous flow with fluid fragmentation of free surfaces. Simulation of fluid fragmentation for collapse of liquid column against an obstacle was carried out. A good agreement was found between the numerical simulation and the available experimental data.

Ye and McCorquodale (1998) simulated curved open channel flows and mass transport using a 3D hydrodynamic model representing free surface turbulent flows. A second order upwind scheme was incorporated to decrease numerical diffusion. The standard $k-\varepsilon$ turbulence model was modified to take into account anisotropic effects that appear in shallow curved channels. To take into account streamline curvature and damping effects of free surface and solid boundaries, algebraic formulations were used for horizontal and vertical eddy viscosities. The model results were in good agreement with the available experimental data.

Maronnier, Picasso and Rappaz (1999) did run the numerical results for two-dimensional free surface flows with the VOF method for several cases. With a PISO algorithm, numerical

results agreed with experimental ones. Again, Maronnier, Picasso and Rappaz (2003) successfully applied VOF methods to three-dimensional free surface flows, and their comparison between the simulation and experimental results was reasonably good.

Huang, Lai and Patel (2001) examined the reliability of the VOF method to solve open channel flow problems. The flow in S-shaped open channels with sloping banks was used as a benchmark, where a three dimensional solver based on the finite volume discretization method was developed and a PISO algorithm was used. They adopted verification and validation procedures to assess numerical uncertainty of the model by comparing it with the experimental results. This study revealed that for the meandering channel flow the overall uncertainties for velocity, water surface elevation, and wall shear stress was estimated to be 3.55%, 5.9% and 20%, respectively. The large error in wall shear stress was restricted to only corner regions.

Mohapatra, Bhallamudi and Eswaran (2001) demonstrated the use of a generalized simplified marker and cell (GENSMAC) flow solver and Young's Volume of Fluid (Y-VOF) surface tracking technique as a valuable tool to study vital mechanics of multiple free surface flows with non-hydrostatic pressure distribution. Numerical results did agree with experimental results for sub-critical and super critical flows.

Three-dimensional numerical modeling was developed by Kocyigit, Falconer and Lin (2002) to predict free surface flows, in which unsteady Reynolds averaged Navier-Stokes equations with non-hydrostatic pressure distribution are used. Hydrodynamic pressure components with prominent effects on velocity fields were considered as test cases. The numerical model produced reasonable results that were in agreement with the experimental ones.

Ramamurthy, Qu and Vo (2005) selected free overfall in a rectangular open channel flow to study the VOF model. A two-dimensional two-equation $k-\varepsilon$ turbulence model using a PISO

(pressure implicit with splitting operators) algorithm with VOF method was used for the simulation. They validated the predictions of a VOF based numerical model using existing experimental and theoretical results for water surface profiles and distributions of the pressure head and velocity components.

Ramamurthy, Qu and Yo (2006) again found good agreement between existing experimental and theoretical results for free surface flow simulation using the VOF method. They applied a three-dimensional two-equation $k-\varepsilon$ turbulence model for simulation of free overfall in a Trapezoidal channel.

In summary, the previous studies on the hydrodynamic loading on a submerged bridge deck showed that the drag, lift and moment coefficients mainly depend on the shape of bridge decks and Froude number; they are more or less independent of Reynolds number and scaling factor. Besides, the VOF method can be used successfully for free surface flow simulations. In the following chapters, we will apply the VOF method by using the commercial software FLUENT to validate the experimental results of hydrodynamic forces on submerged bridge decks. FLUENT software will also be used to examine the scaling effect on the drag, lift and moment coefficients.

Chapter 3 Methodology used in Simulations

The drag coefficient C_D , lift coefficient C_L , and moment coefficient C_M are defined as:

$$C_D = \frac{\sum F_x}{\frac{1}{2} \rho v^2 (Ls)} \quad \text{if } h^* > 1 \quad \text{where,} \quad h^* = \frac{h_u - h_b}{s}$$

$$C_D = \frac{\sum F_x}{\frac{1}{2} \rho v^2 [L(h_u - h_b)]} \quad \text{if } h^* < 1$$

$$C_L = \frac{\sum F_y}{\frac{1}{2} \rho v^2 (LW)}$$

$$C_M = \frac{(\sum \vec{r} \times \vec{F}) \cdot \hat{k}}{\frac{1}{2} \rho v^2 (LW^2)}$$

where,

$\sum F_x$ = Force integrated over the surface of a bridge deck along the flow direction

$\sum F_y$ = Force integrated over the surface of a bridge deck perpendicular to the flow direction

h^* = inundation ratio

h_u = depth of flow

h_b = height from bottom of the flume to bottom of bridge

s = bridge deck height

ρ = density of water

V = Flow velocity

L = Length of the bridge velocity

W = Width of the bridge.

When calculating the integrated vertical force, ΣF_Y , over the bridge deck for lift, its component associated with buoyancy force was excluded from the sum to be consistent with the experiments in which force balances were calibrated for zero lift under no-flow conditions.

In order to analyze the effect of scale on drag, lift and moment coefficients on an inundated bridge deck, four CFD models scaled to a factor of 1:1.5, 1:1, 3:1 and 5:1 were setup for numerical simulations. The boundary conditions were setup according to the Froude number similarity, hence they met the requirements of the geometric similarity and the Froude number similarity. However, the model was distorted because they did not meet the requirements of the Reynolds number similarity. The aim of the numerical simulation was to check the difference of non-dimensional hydrodynamic forces acting on a bridge deck when the simulation results of the small sized model was used to predict the situations of the large sized model according to the similitude theory.

The three-dimensional computational fluid dynamic model was used to test the scale effects on non-dimensional hydrodynamic forces acting around on the bridge deck. The commercially available software, Fluent, was used to run the simulations, and Gambit was used to generate the grid of the computational domain. The nodes can be placed accordingly within the computational domain depending on the shape of the body in unstructured mesh, therefore tetrahedral cells were generated. The grid near the bridge deck was denser because the flow pattern in the region is more complex and gradually increases away from the bridge deck. The boundary conditions were: inlet as velocity inlet, outlet as pressure outlet, bottom of the channel and bridge deck as non-slip wall, and top of the channel as pressure outlet.

A uniform velocity in accordance with the experiment was applied on the inlet boundary corresponding to Froude number of 0.32 and at the outlet boundary zero pressure gradients were set (i.e., the variables at downstream end are extrapolated from the interior domain). The simulations were completed using Volume of Fluid (VOF) multiphase model and $k-\varepsilon$ turbulence models. To obtain a good convergence, the time step size was set to 0.01 seconds with 20

iterations per time step. The simulations were run for 400 seconds and the convergence of the drag, lift and moment coefficient was monitored with time. Due to the fluctuating values of drag, lift and moment coefficients, the average value was used. The parameters in operating conditions were the same in all of the cases. The operating pressure was set as the atmospheric pressure: that is, 101325 Pascal. The gravitational acceleration was set in y-direction as -9.81 m/s^2 and the operating density was set as 1.225 kg/m^3 .

To obtain results more accurately, the discretization scheme for pressure was set as Body Force Weighted, and second order upwind scheme was used for other terms like momentum, volume fraction and turbulent kinetic energy. The under relaxation parameters were set to 0.3 for pressure, and 0.7 for density, momentum, turbulent kinetic energy, and turbulent dissipation rate. The reference value for each case was setup based on the dimensions of the bridge deck model used. The residuals for convergence were set to 10^{-6} for continuity equation, turbulence kinetic energy and turbulence dissipation rate. The dimensions of the rectangular channel and the geometrical setup used in each numerical simulation are shown in figures 3-1 to 3-10.

CASE A: Scaled 1:1

The three-dimensional CFD model was scaled to a factor of 1:1—the same dimensions as the experimental setup. The rectangular channel was 6.5 m long, 0.356 m wide and 0.5 m height (as shown in Fig. 1.1). The bridge deck was located 4.6 m downstream from the inlet of the channel and a uniform velocity of 0.51 m/s was set at the inlet. The depth of flow was kept constant at 0.25 m, and the height of the bridge deck from the bottom of the channel (h_b) was set as 60 mm, 100 mm, 130 mm, 160 mm, 180 mm, 200 mm and 220 mm to attain the various flooding heights. The dimensions of the bridge deck used in the simulations were the same as in the experimental setup (Fig. 3.2). The grid of the simulation generated by Gambit is shown in

figure 3.3. The grid near the bridge was generated more densely because the flow in the region is more complex. A multi-block grid generation technique was used for the goal. The grid cells near the bridge deck were around 3 mm and gradually increased to size of 2 cm away from the bridge deck. A three-dimensional grid system with 227,428 nodes and 1,122,818 cells was generated with GAMBIT. The grid consisted of two zones: water and air. Through the transient simulation, using VOF multiphase model, the water flows in the open channel and constitutes the free surface between air and water for the specified inlet and outlet conditions.

Reference values used in numerical simulations:

- Projected area for drag coefficient = 0.0198 m^2
- Projected area for lift and moment coefficient = 0.088 m^2
- Length = 26 cm, Upstream velocity = 50 cm/s.

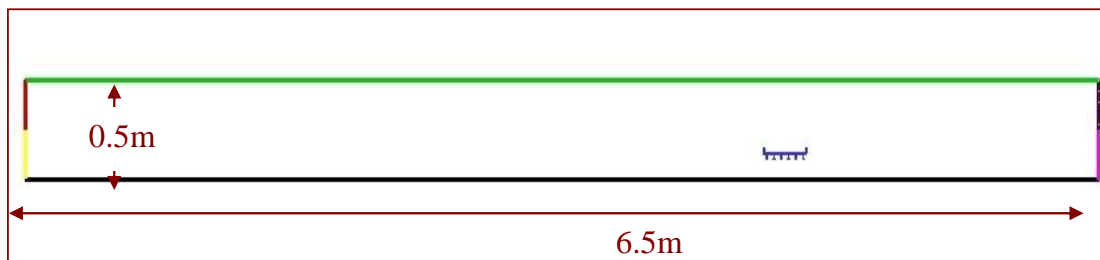


Figure 3.1 Dimensions of the Experimental Setup and CFD Model Scaled 1:1

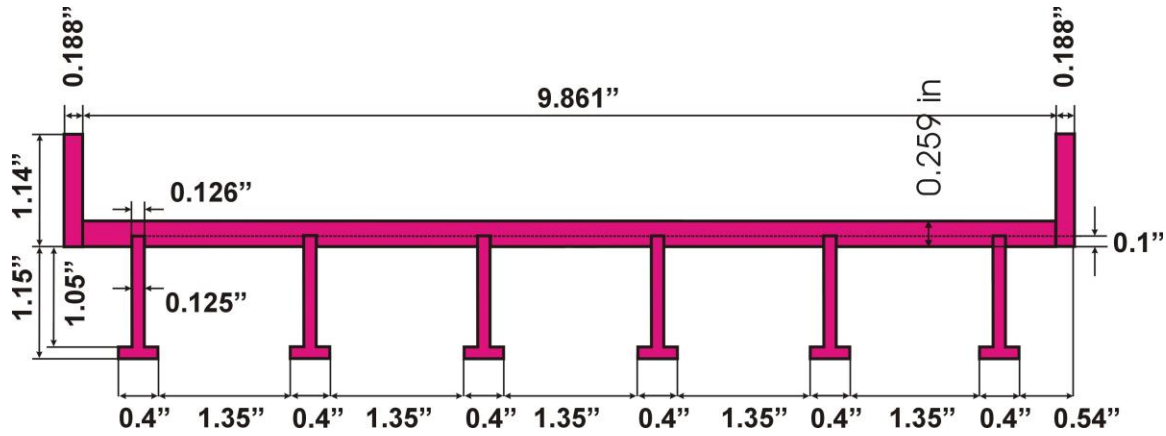


Figure 3.2 Dimension of Prototype Six-Girder Bridge Deck Model used in Experiments and CFD

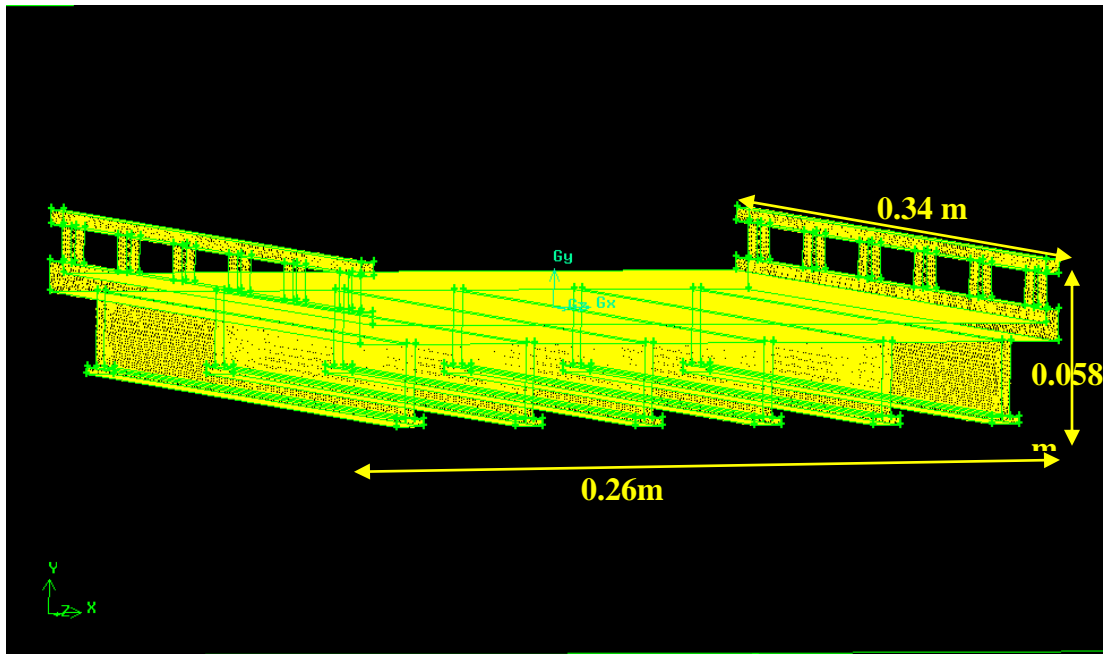


Figure 3.3 Meshed Geometry of Six-Girder Bridge Deck Model used in CFD (1:1)

CASE B: Scaled 1:1.5 (smaller)

The three-dimensional CFD model was scaled to a factor of 1:1.5, or 1.5 times smaller than the experimental setup. The rectangular channel was 4.5 m long, 0.24 m wide and 0.3 m in height (Fig. 3.4). The dimensions of the bridge deck used in the simulations were 1.5 times

smaller than the one used in the experimental setup, as shown in figure 3.5. The bridge deck was located 3.1 m downstream from the inlet of the channel, and a uniform velocity of 0.4 m/s was set at the inlet with a corresponding Froude number of 0.32. The depth of flow was kept constant at 0.167 m, and the height of the bridge deck from the bottom of the channel (h_b) was set as 40 mm, 68 mm, 86 mm, 106 mm, 120 mm, 140 mm and 155mm to get the various flooding heights. The grid cells near the bridge deck were around 1.5 mm and gradually increasing to size of 1 cm away from the bridge deck. A three-dimensional grid system with 383,665 nodes and 1,847,801 cells was generated with GAMBIT.

Reference values used in numerical simulations:

- Projected area for drag coefficient = 0.00891 m²
- Projected area for lift and moment coefficient = 0.0398 m²
- Length = 17.3 cm, Upstream velocity = 35 cm/s.

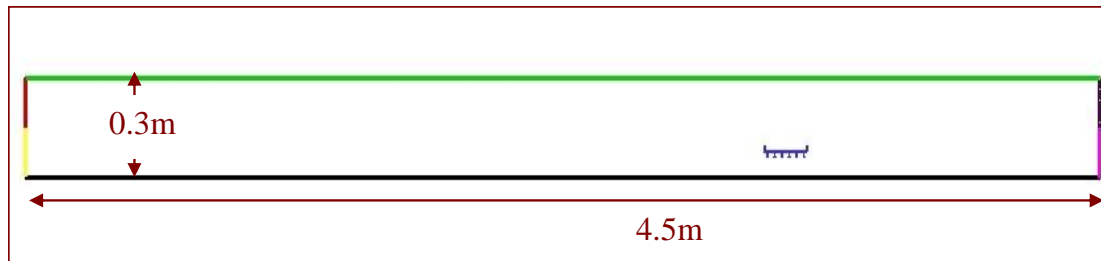


Figure 3.4 Dimensions of the Experimental Setup and CFD Model Scaled by 1:1.5 (Smaller)

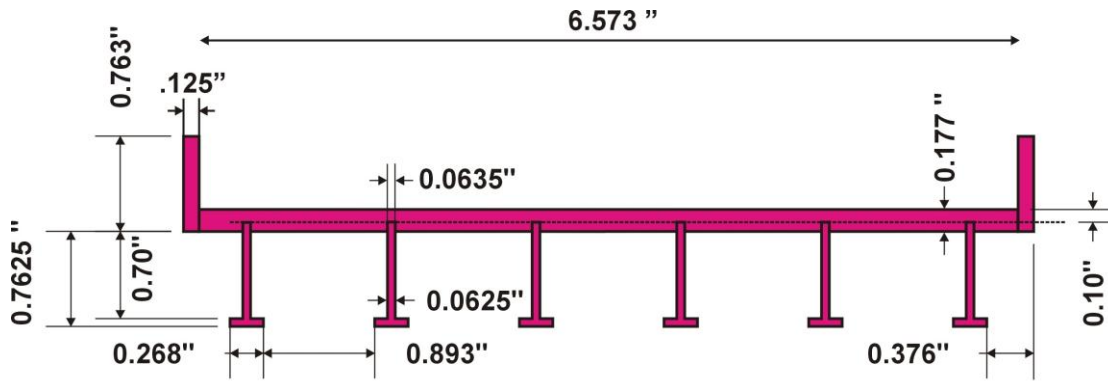


Figure 3.5 Dimensions of the CFD Model Scaled by 1:1.5 (Smaller)

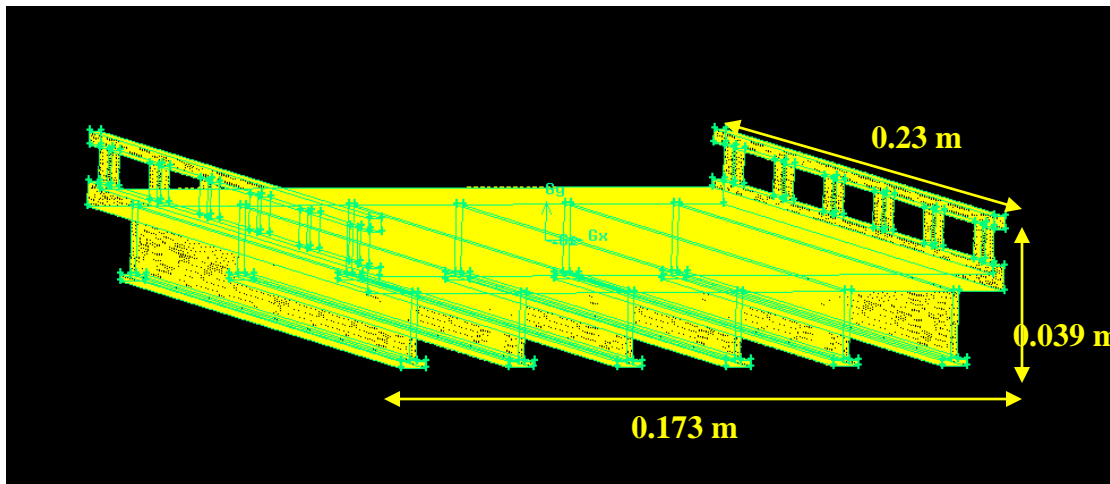


Figure 3.6 Meshed Geometry of Bridge Deck used in CFD Scaled by 1:1.5 (Smaller)

CASE C: Scaled 3:1 (bigger)

The three-dimensional CFD model was scaled to a factor of 3:1, or three times bigger than the experimental setup. The rectangular channel was 19.5 m long, 1.068 m wide and 1.2 m high (Fig. 3.7). The dimensions of the bridge deck used in the simulations were three times bigger than that in the experiments. The bridge deck was located 13.8 m downstream from the inlet of the channel, and a uniform velocity of 0.866 m/s was set at the inlet. The depth of flow was kept constant at 0.75 m, and the height of the bridge deck from the bottom of the channel

(h_b) was used as 180 mm, 300 mm, 390 mm, 480 mm, 540 mm, 600 mm, 660 mm and 690 mm to get the various flooding heights.

The grid cells near the bridge deck were around 2 cm and gradually increasing to size of 4 cm away from the bridge deck. A three-dimensional grid system with 343,551 nodes and 1,839,577 cells was generated with GAMBIT.

Reference values used in numerical simulations:

- Projected area for drag coefficient = 0.181 m^2
- Projected area for lift and moment coefficient = 0.795 m^2
- Length = 78 cm, Upstream velocity = 86.6 cm/s.

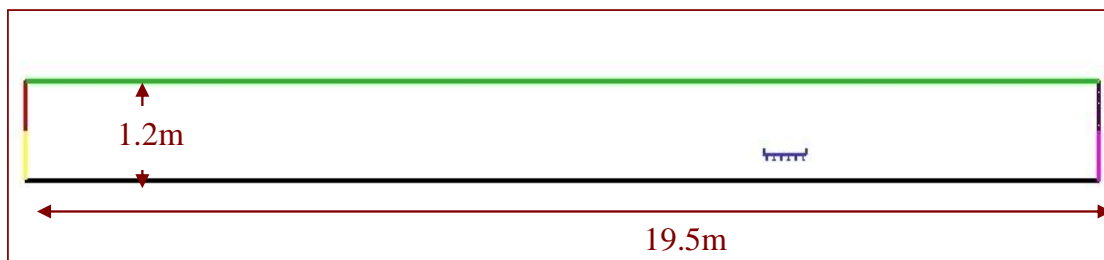


Figure 3.7 Dimensions of the CFD Model Scaled 3:1 (Bigger)

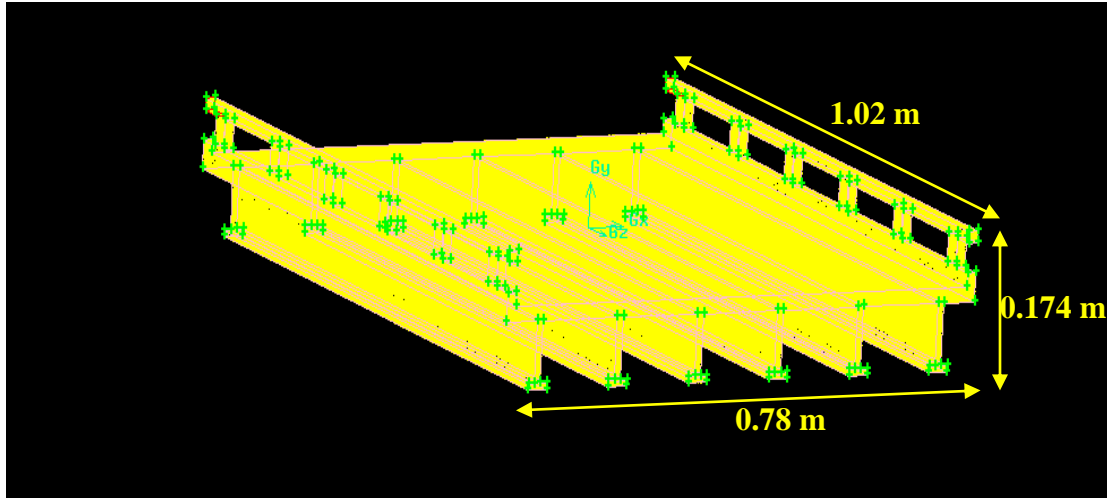


Figure 3.8 Meshed Geometry of Bridge Deck used in CFD Scaled by 3:1 (Bigger)

Case D: Scaled 5:1 (bigger)

The three-dimensional model used in the numerical simulations was scaled to a factor of 5:1 times bigger than the experimental setup. The rectangular channel was 23.5 m long, 0.356 m wide and 2 m high (Fig. 3.9). The bridge deck was located 23m downstream from the inlet of the channel, and a uniform velocity of 1.14 m/s was set at the inlet. The depth of flow was kept constant at 1.25 m, and the height of the bridge deck from the bottom of the channel (h_b) was 300 mm, 500 mm, 650 mm, 800 mm, 900 mm, 1000 mm, 1100 mm and 1150 mm to get the various flooding heights. The dimensions of the bridge deck used in the simulation were scaled by a factor of 5:1, which is 5 times bigger than that in the experiments. The grid cells near the bridge deck were around 4 cm and gradually increased to size of 7 cm away from the bridge deck. A three-dimensional grid system with 778,703 nodes and 3,820,274 cells was generated with GAMBIT.

Reference values used in numerical simulations:

- Projected area for drag coefficient = 2.21 m²

- Projected area for lift and moment coefficient = 0.504 m^2
- Length = 130 cm, Upstream velocity = 114 cm/s.

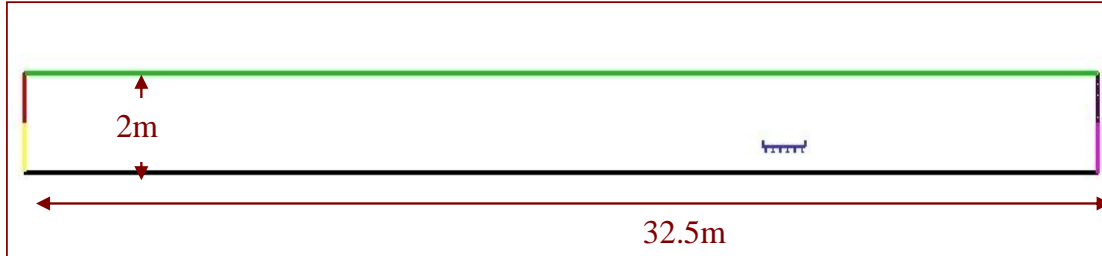


Figure 3.9 Dimensions of the CFD model scaled by 5:1 (bigger).

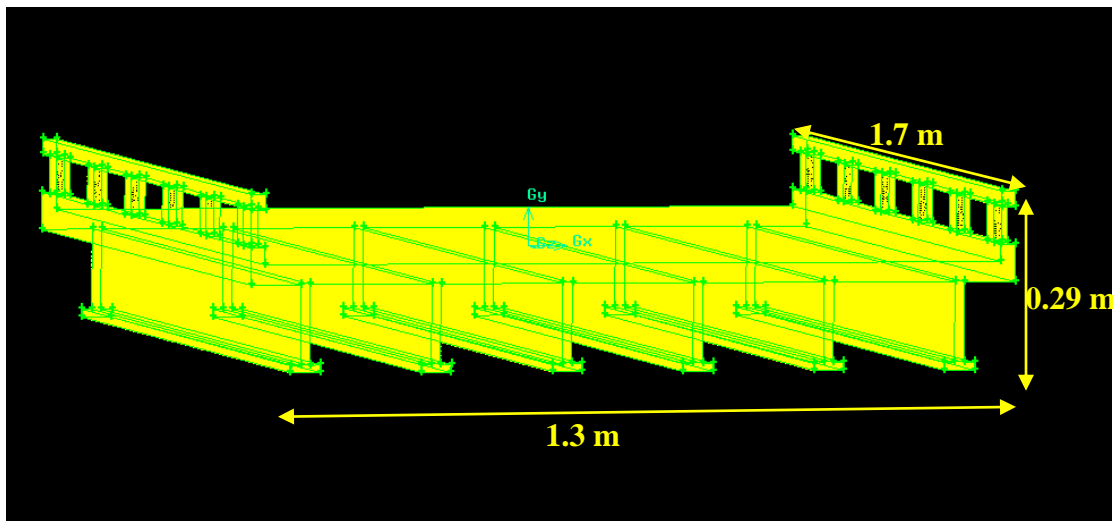


Figure 3.10 Meshed Geometry of Bridge Deck Model used in CFD Scaled by 5:1 (Bigger)

The depth of flow, h_u , for all cases was kept constant, and the height of the bridge deck, h_b , was varied to get the different inundation ratios of 0.86, 1.2, 1.55, 2.06, 2.5, and 3.2. The CFD results for the bridge deck were initially validated with the experimental data, and the methodology was used to simulate the hydrodynamic forces on the scaled bridge decks.

Chapter 4 Results and Analysis

4.1 Drag, Lift and Moment Coefficients

A combined experimental and computational study on inundated bridge discussed earlier was recently completed. The study was done in collaboration among the FHWA Hydraulics lab, the Transportation Research Analysis and Computing Center (TRACC) at Argonne National Laboratory, and the University of Nebraska-Lincoln. The study showed that drag, lift and moments on inundated bridge decks in laboratory settings can be accurately predicted using commercially available Computational Fluid Dynamics software, FLUENT, with either a $k-\varepsilon$ model or large eddy simulation (LES). The validated CFD methodology was applied to predict the effects of scale on non-dimensional hydrodynamic forces. In order to compare the simulation results with experiment results, all of the data is plotted in dimensionless form. The combination of variables was the same as that used in the experiments. Since LES requires longer computational times and large CFD models scaled to 3:1 and 5:1 will require significantly high computational time, the numerical simulations for scaled bridge decks were done using the $k-\varepsilon$ turbulence model. The CFD models were run for 400 seconds with a time step size of 0.01s and 20 iterations per time step. Due to fluctuating values of C_D and C_L with time, the final values of C_D , C_L , and, C_M are averaged from 150 to 400 seconds. The 3:1 scaled CFD model simulations were completed in about 130 hours of wall-clock time using 16 processors, and a 5:1 scaled bridge deck model took a wall clock time of around 180 hours using 16 processors.

The results of the numerical simulations of flow around a small and large size bridge deck are plotted in figures 4.1, 4.2 and 4.3. Initially to study the effect of scaling, the numerical simulations were completed for a bridge deck scaled 1:1.5, which is 1.5 times smaller than the prototype. After validating the results of the smaller bridge deck with the prototype, the large

size bridge decks (i.e., 3:1 and 5:1) was completed. The effect of scaling on non-dimensional hydrodynamic forces—drag, lift and, moment coefficients—were investigated by comparing different results obtained from a scaled numerical model derived from the Froude number similarity method.

The drag coefficient plot for prototype and scaled bridge deck is shown in figure 4.1, which shows the drag coefficient is positive at all values of h^* . The minimum value of drag coefficient was found at h^* around 0.5 – 0.8, which corresponds to a case when the bridge is inundated slightly more than halfway, perhaps as the water level reaches the top of girders and begins to transition to overtopping the deck. As the bridge becomes more inundated ($h^* > 1.5$), the drag coefficient values level off to around two. Consequently, for a certain inundated condition of a bridge deck, C_D will be free to the influence of free surface and the channel bottom. The drag coefficient results for scaled bridge deck show a similar trend as the prototype, the drag coefficient, initially increases and then stays constant. The drag coefficient for scaled bridge deck and prototype are at a higher inundation ratio ($h^* > 1.5$), which means that the bridge is completely submerged and was found to be approximately 2.2. The scaled bridge decks did not show any significant effect of scaling since the difference between the drag coefficient for the small and large size bridge deck was small. The results of the flow field distribution around the small and large size bridge deck model was also found to be very similar, which is discussed later in this chapter.

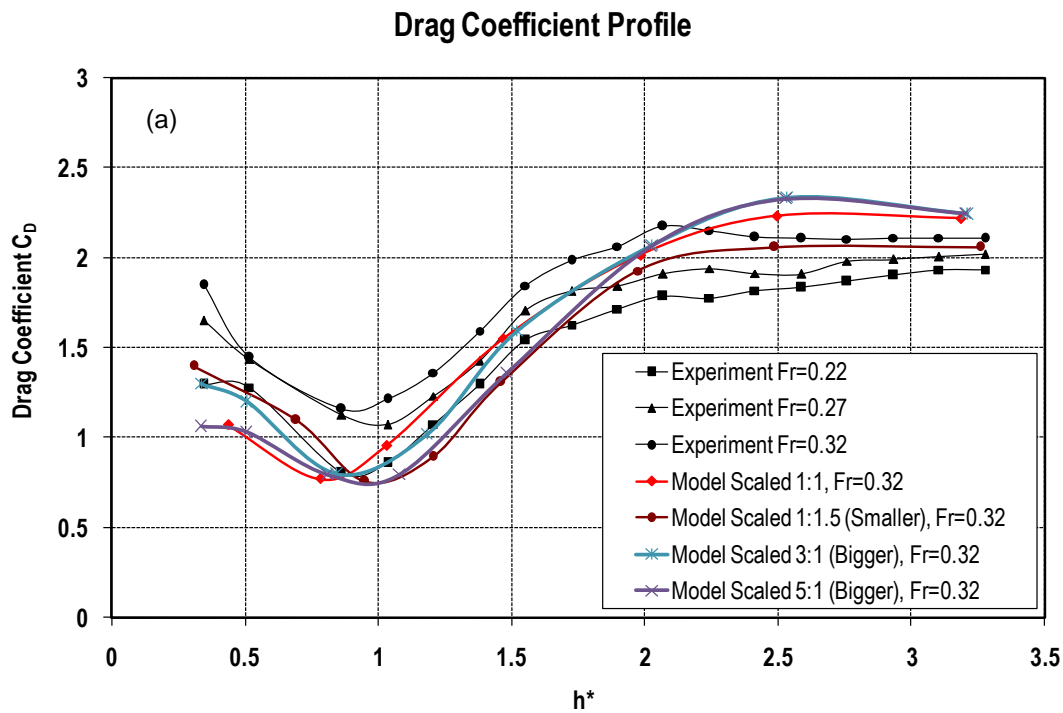


Figure 4.1 Drag Coefficients for Scaled and Prototype Six-Girder Bridge Deck

Figure 4.2 shows the variation of simulated lift coefficient values with h^* for various scaled bridge decks and the prototype. To be consistent with the experiments, the component of buoyancy was subtracted from the lift force for all of the cases. After subtracting the buoyancy force from the lift force, the lift coefficient comes out to be negative. A negative lift coefficient means that the flow is actually exerting a pull-down force on the bridge. While the effect is quite small when the water level just barely reaches the bottom of the girders, the lift coefficient rapidly becomes more negative until h^* roughly equals 0.65. The lift coefficient slowly returns to zero as the inundation ratio exceeds three. The CFD results for the lift coefficient agree with the experimental data at higher inundation ratios but deviations from the experimental data can be seen at a lower inundation ratio. As h^* decreases (as it gets more negative), the lift coefficient value for a scaled bridge deck decreases and is influenced by both the free surface and channel

bottom. The CFD results for scaled bridge deck agree with the measurements of the prototype at a higher inundation ratio, but do not closely follow the experimental results at a lower inundation ratio. The entire scaled bridge deck models follow a similar trend, showing some influence from the inundation ratio. The lift coefficient results do not show any significant scale effect for the bridge deck scaled to a factor of 1:1 and 3:1. However, looking at the smallest scale (1:1.5) and the largest scale (5:1) an overall difference of approximately 15% has been observed in the lift coefficient values—showing some effect of scaling. This may be because only Froude number similarity was met, the Reynolds number similarity was neglected and the model was distorted.

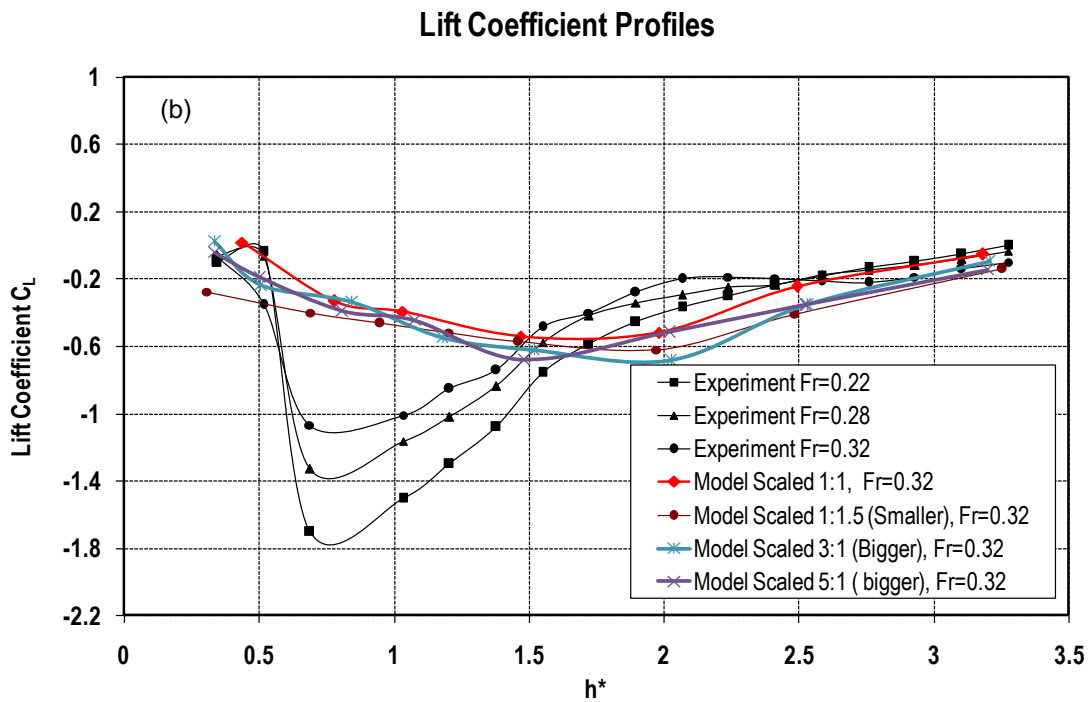


Figure 4.2 Lift Coefficient Scaled and Prototype Six-Girder Bridge Deck

Figure 4.3 shows that when h^* increases to 1, the moment coefficient increases and becomes more negative with an increasing inundation ratio, which indicates that the free surface

wave force is the source of the moment coefficient. The moment coefficient for scaled bridge deck and prototype closely follow each other, thus showing a similar trend. The maximum moment coefficient was observed when the bridge was roughly halfway submerged and the flow was pushing almost entirely on the first girder and thus below the center of gravity. The moment coefficient for the small and large size bridge-decks were found to be very close to each other and did not show any effect of scaling. The CFD results of moment coefficient for both prototype and the scaled bridge deck do not closely follow the experimental data at lower inundation ratio.

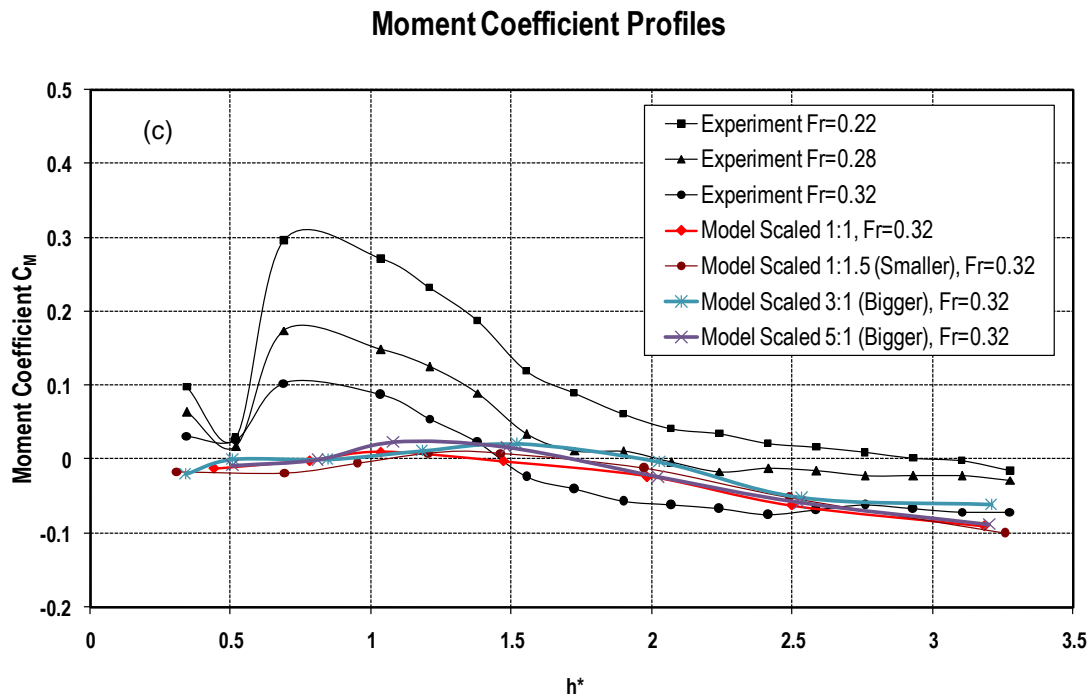


Figure 4.3 Moment Coefficient for Scaled and Prototype Six-Girder Bridge Deck

Table 4.1 CFD Results of C_D , C_L and, C_M for Scaled Bridge Decks

h_b (m)	h_u (m)	h^*	V (m/s)	C_D	C_L	C_M
Prototype 1:1						
0.06	0.25	3.18	0.50	2.22	-0.05	-0.09
0.10	0.25	2.50	0.50	2.23	-0.25	-0.06
0.13	0.25	1.98	0.50	2.02	-0.52	-0.02
0.16	0.25	1.47	0.50	1.55	-0.54	0.00
0.18	0.24	1.03	0.50	0.96	-0.40	0.01
0.20	0.25	0.78	0.50	0.77	-0.33	0.00
0.22	0.25	0.44	0.50	1.07	0.02	-0.01
Scaled 1.5 : 1 (Smaller)						
0.04	0.17	3.26	0.40	2.06	-0.14	-0.10
0.07	0.17	2.49	0.40	2.06	-0.41	-0.05
0.09	0.17	1.97	0.40	1.93	-0.62	-0.01
0.11	0.17	1.46	0.40	1.31	-0.57	0.01
0.12	0.17	1.21	0.40	0.90	-0.52	0.01
0.13	0.17	0.95	0.40	0.76	-0.46	-0.01
0.14	0.17	0.69	0.40	1.10	-0.40	-0.02
0.16	0.17	0.31	0.40	1.40	-0.28	-0.02
Scaled 1 : 3 (Bigger)						
0.18	0.75	3.21	0.87	2.24	-0.09	-0.06
0.30	0.75	2.53	0.87	2.34	-0.35	-0.05
0.39	0.75	2.03	0.87	2.07	-0.68	0.00
0.48	0.75	1.52	0.87	1.59	-0.62	0.02
0.54	0.75	1.18	0.87	1.02	-0.55	0.01
0.60	0.75	0.84	0.87	0.80	-0.34	0.00
0.66	0.75	0.51	0.87	1.20	-0.24	0.00
0.69	0.75	0.34	0.87	1.30	0.02	-0.02
Scaled 1 : 5 (Bigger)						

0.30	1.25	3.20	1.14	2.25	-0.15	-0.09
0.50	1.25	2.53	1.14	2.33	-0.36	-0.06
0.65	1.25	2.02	1.14	2.06	-0.52	-0.02
0.80	1.24	1.48	1.14	1.36	-0.68	0.02
0.90	1.22	1.08	1.14	0.80	-0.45	0.02
1.00	1.24	0.81	1.14	0.80	-0.39	0.00
1.10	1.25	0.51	1.14	1.03	-0.19	-0.01
1.15	1.25	0.34	1.14	1.06	-0.04	-0.01

4.2 Contour Plots for Variables around Scaled Bridge Decks

4.2.1 Velocity Distribution

The velocity contours around the bridge deck for the scaled bridge decks and the prototype are plotted for the case of $Fr = 0.32$ in figures 4.4 (a) to 4.4 (d). The velocity contours are plotted at a simulation time of 300 seconds. The velocity contours illustrate that the contraction occurs. For instance, the pressure flow is separated by the bridge deck, resulting in the increase of flow velocity under the bridge deck. The experiments using PIV also showed similar velocity distribution around the bridge deck. The predicted velocity distribution around the bridge deck for the prototype and the scaled bridge deck is very similar, showing a pressure flow under the bridge deck and low or negative velocities between and under the girders. These low and negative velocities possibly influence the stability of the bridge deck and it is important to minimize the region of negative velocities.

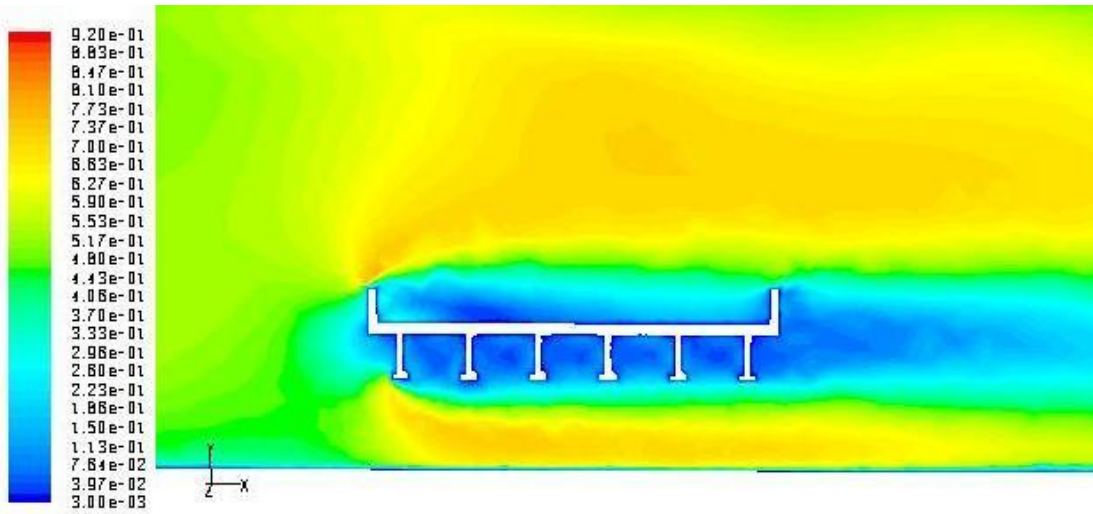


Figure 4.4(a) Velocity Distribution for Prototype

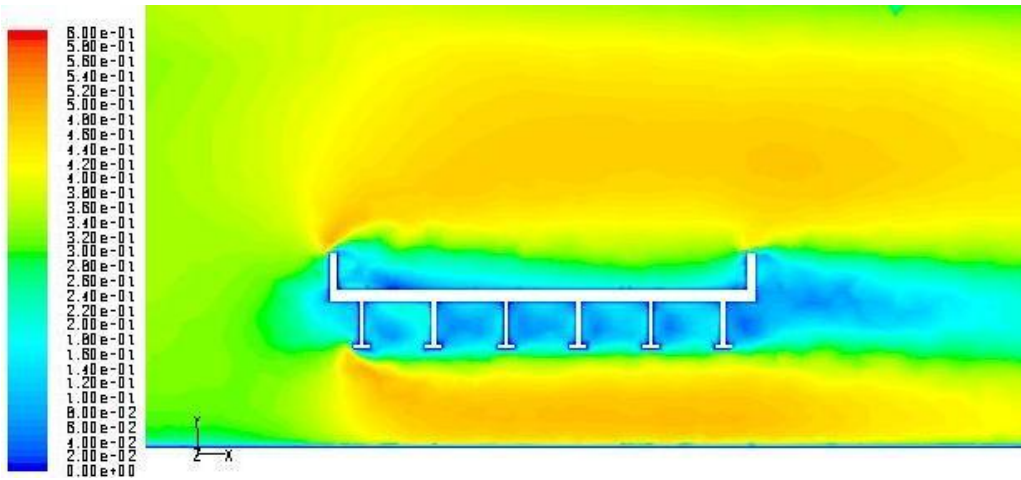


Figure 4.4(b) Velocity Distributions for 1.5:1

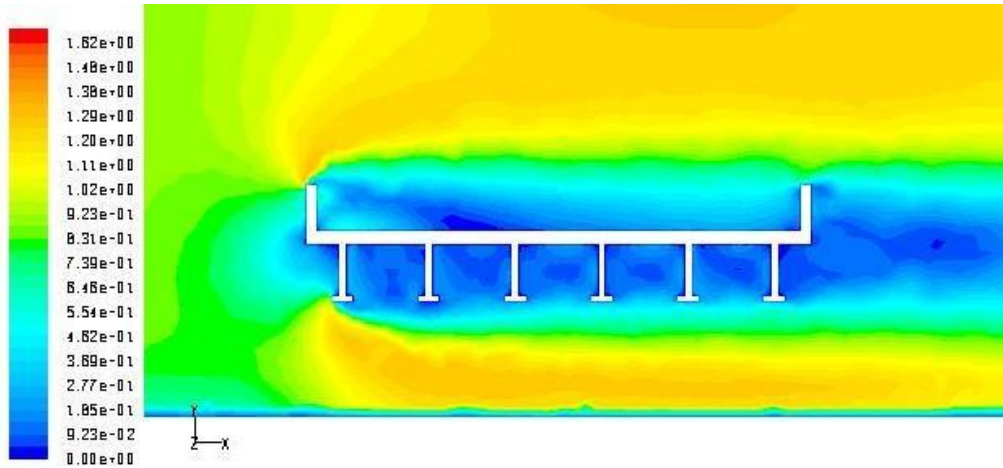


Figure 4.4(c) Velocity Distribution for 1:3

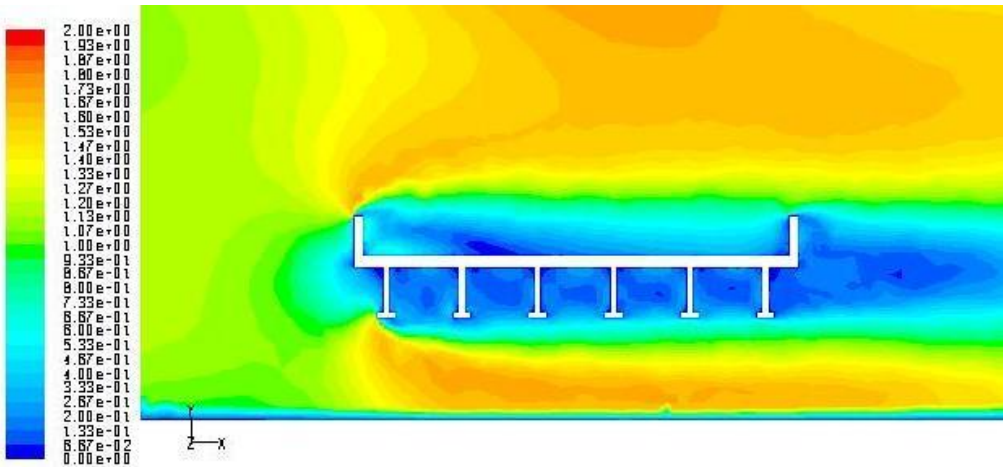


Figure 4.4(d) Velocity Distributions for 1:5

4.2.2 Pressure distribution

Figures 4.5 (a) to 4.5 (d) illustrate the contours of dynamic pressure distribution on the surface of the bridge as well as around the scaled bridge deck models and the prototype. The dynamic pressure is related to the kinetic energy of a fluid particle since both quantities are proportional to the particle's mass (through the density, in the case of dynamic pressure) and square of the velocity. If the fluid density is constant, dynamic pressure is proportional to the square of the particle's velocity. The contours are plotted for completely a submerged case when the front of the bridge deck has the maximum impact of the dynamic pressure. However, for a

partially submerged case, a small region of the surface of bridge deck is affected by the high dynamic pressure. The contours of dynamic pressure correspond to a inundation ratio of 3 and Froude numbers such as 0.32. The prototype and scaled bridge deck illustrate similar pressure distribution around the bridge deck, showing that pressure distribution depends on the shape of the object and is independent of the scale. As expected, the overall magnitude of the pressure was smaller in the case of the 1.5:1 scaled bridge deck and had higher magnitude in the case of the 1:5 scaled bridge deck, but overall showed similar distribution. The drag and lift force is the resultant force due to shear stress and pressure distribution on bridge deck. The higher pressure on the upstream face when water hits the bridge deck and low pressure at the downstream face can lead to instability or failure of bridge.

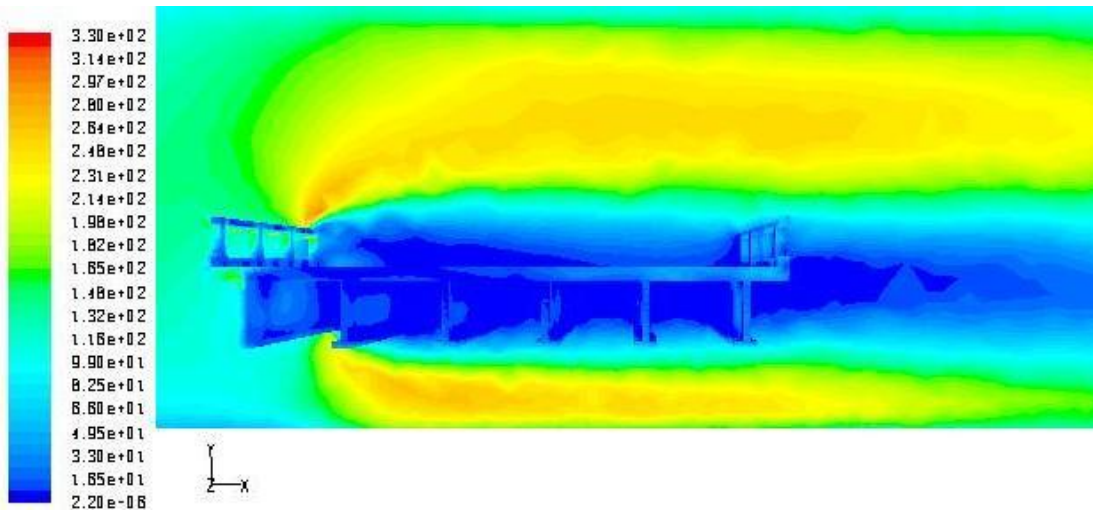
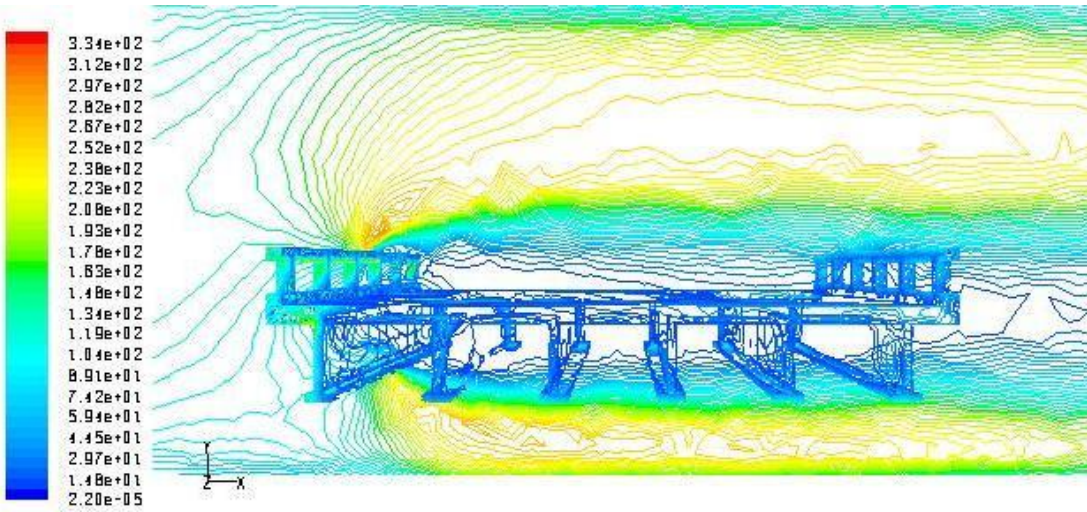


Figure 4.5(a) Pressure Distribution around Prototype 1:1 Bridge Deck

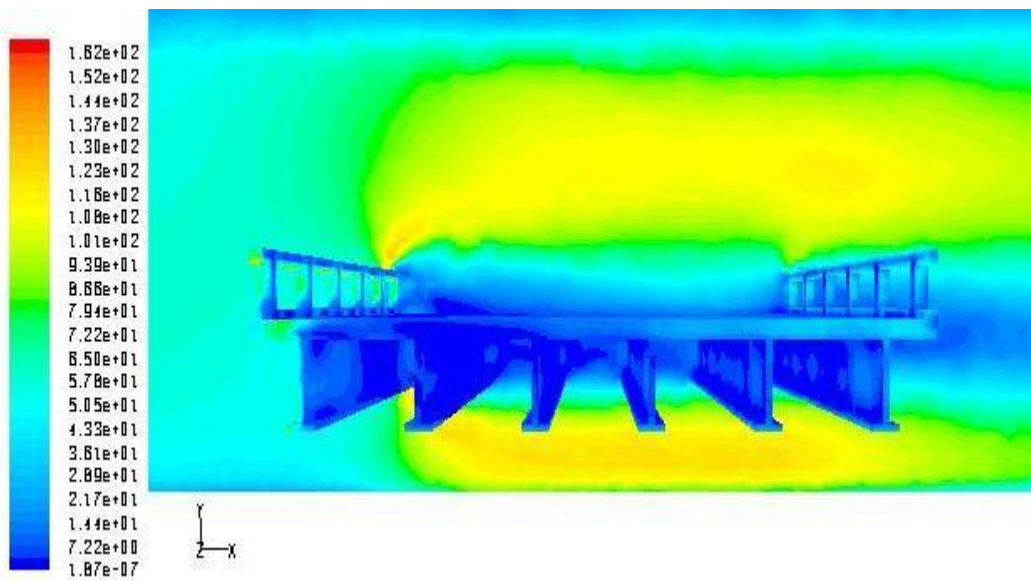
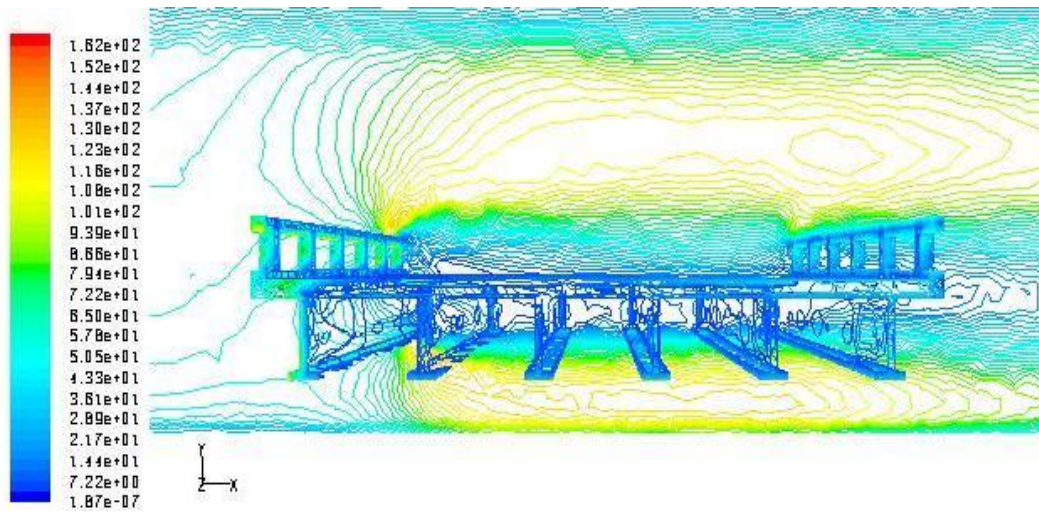


Figure 4.5(b) Pressure Distribution for 1.5:1 Scaled Bridge Deck

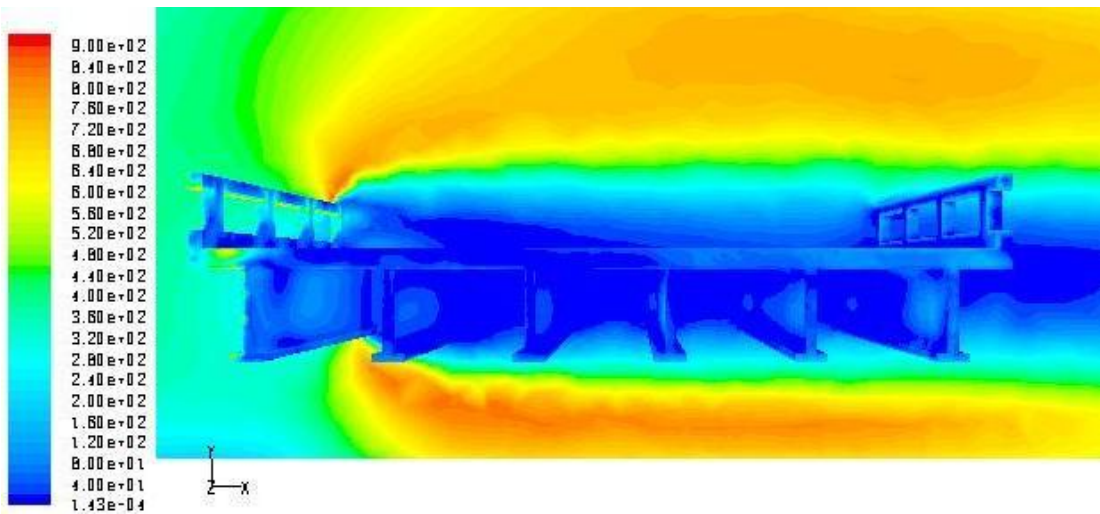
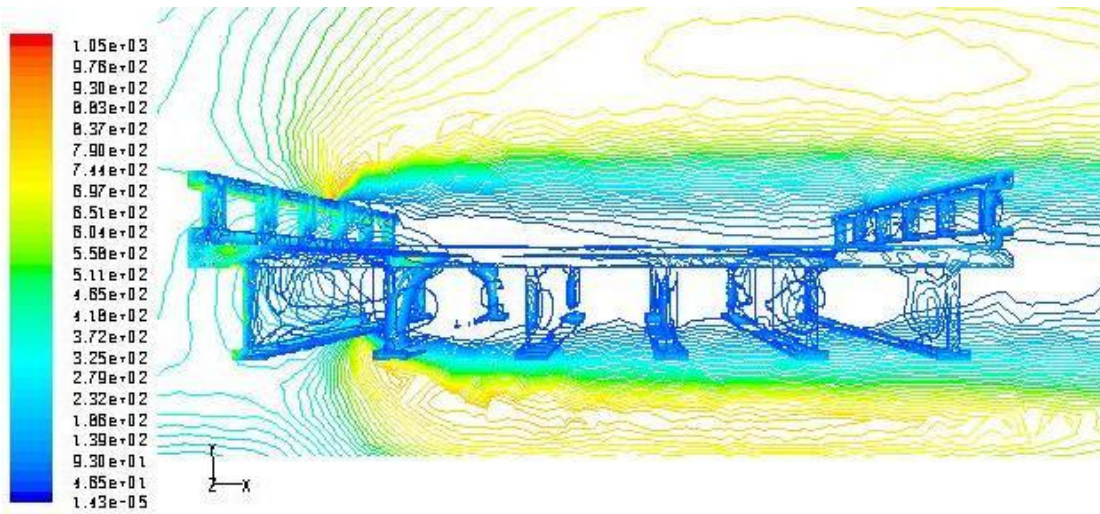


Figure 4.5(c) Pressure Distribution for 1:3 Scaled Bridge Deck

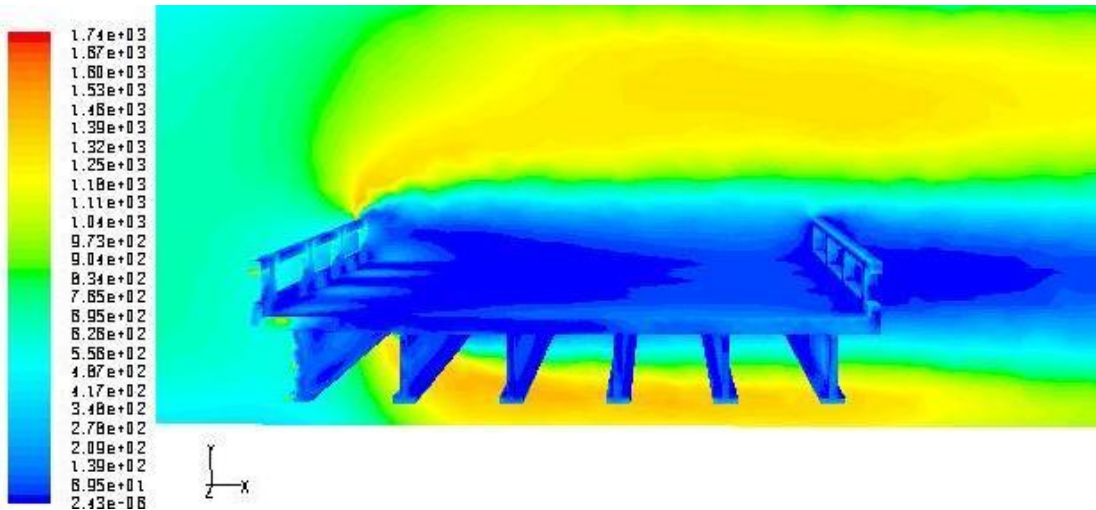
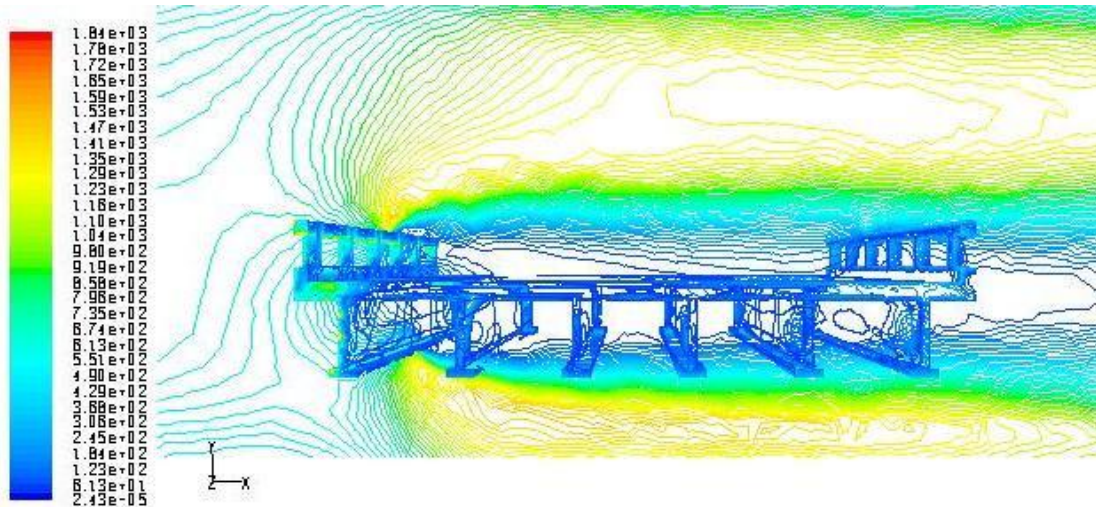


Figure 4.5(d) Pressure Distribution for 1:5 Scaled Bridge Deck

4.2.3 Turbulence kinetic energy

The turbulence kinetic energy (TKE) is the mean kinetic energy per unit mass associated with eddies in turbulent flow and is characterized by measured root-mean-square (RMS) velocity fluctuations. Turbulence kinetic energy is based on the turbulence model used, which is from the $k-\epsilon$ turbulence model in the present study. TKE can be due to the shear, friction or buoyancy, or through external forcing at low-frequency eddy scales produced by fluid. Turbulence kinetic

energy is then transferred down the turbulence energy cascade, and is dissipated by viscous forces at the Kolmogorov scale.

Figures 4.6 (a) to 4.6 (d) show the turbulence kinetic energy distribution around the prototype and the scaled bridge deck model. The turbulence kinetic energy was obtained from the $k-\varepsilon$ turbulence model and the simulations were done for completely submerged bridge deck corresponding to Froude number 0.32. The maximum turbulence kinetic energy is at the point of separation when the high velocity flow hits the bridge deck and further decays. The region with green color around the bridge deck is the region with higher turbulence kinetic energy, showing the maximum fluctuations around the bridge deck. The maximum value of the turbulence kinetic energy in the case of smallest bridge deck (scaled to 1:1.5) is around 0.025 and the largest bridge deck (scaled to 5:1) is around 0.7. Since the velocity is higher in the case of a large bridge deck leading to higher fluctuations, both prototype and the scaled bridge deck show similar distribution of turbulence kinetic energy around the bridge deck.

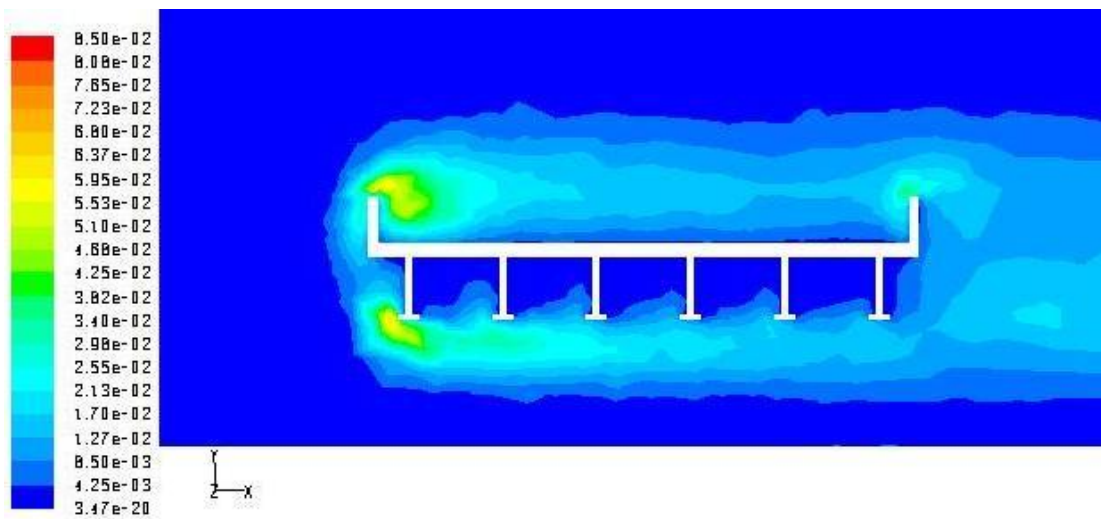


Figure 4.6(a) Contours of Turbulence Kinetic Energy Distribution around the Bridge for Prototype

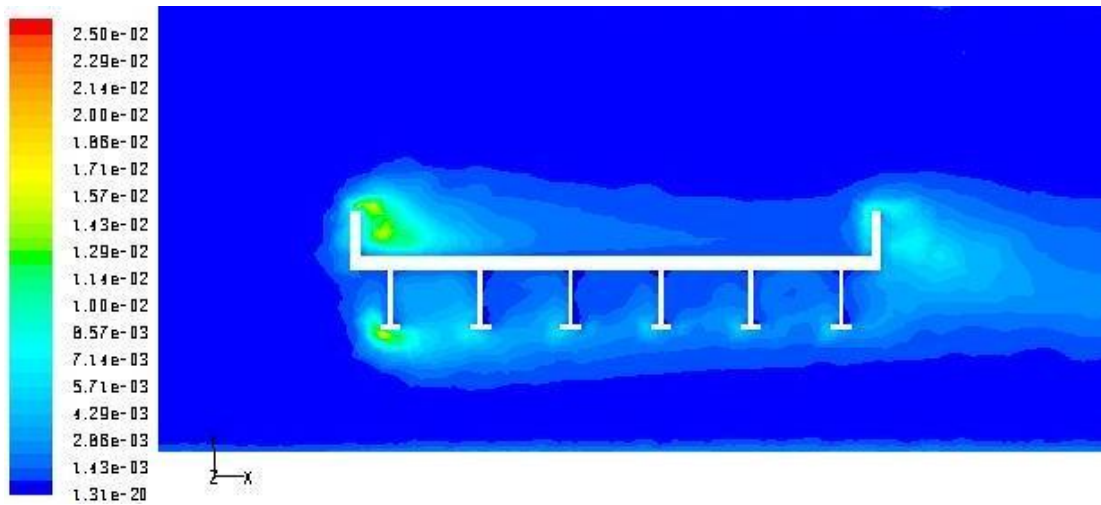


Figure 4.6(b) Contours of Turbulence Kinetic Energy Distribution around the 1.5:1 Scaled Bridge Deck

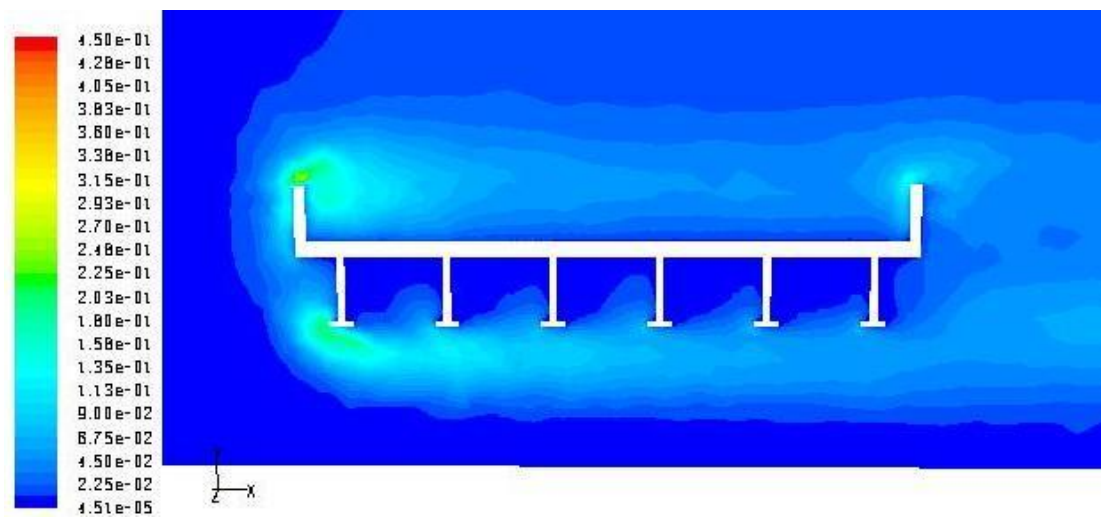


Figure 4.6(c) Contours of Turbulence Kinetic Energy Distribution around the 1:3 1 Scaled Bridge Deck

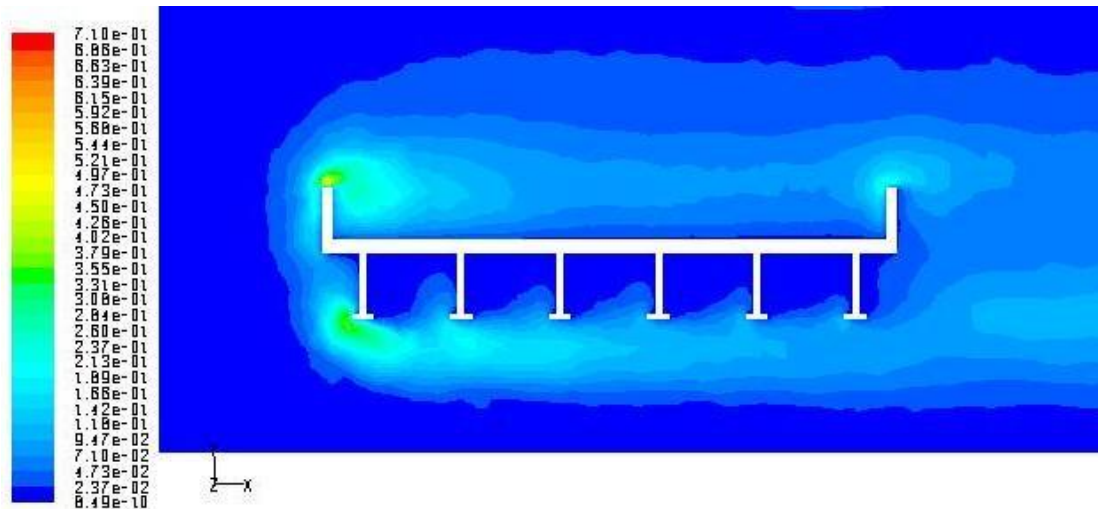


Figure 4.6(d) Contours of Turbulence Kinetic Energy Distribution around the 1:5 1 Scaled Bridge Deck

4.2.4 Turbulence dissipation rate

Accurate estimation of the turbulence dissipation rate is important for the turbulent flows. The turbulence dissipation is higher at the front edge, rear edge and girders of the bridge deck (Fig. 4.7 (a) to 4.7 (d)). The maximum dissipation was observed at the front edge of the bridge deck and at the first girder facing the flow, where the magnitude of turbulence fluctuations is also higher. The magnitude of turbulence dissipation for a 1:5 scaled bridge was found to be ten times more than the 1.5:1 scaled bridge deck model. The scaled bridge deck model and the prototype illustrate similar distribution of the turbulence dissipation rate.

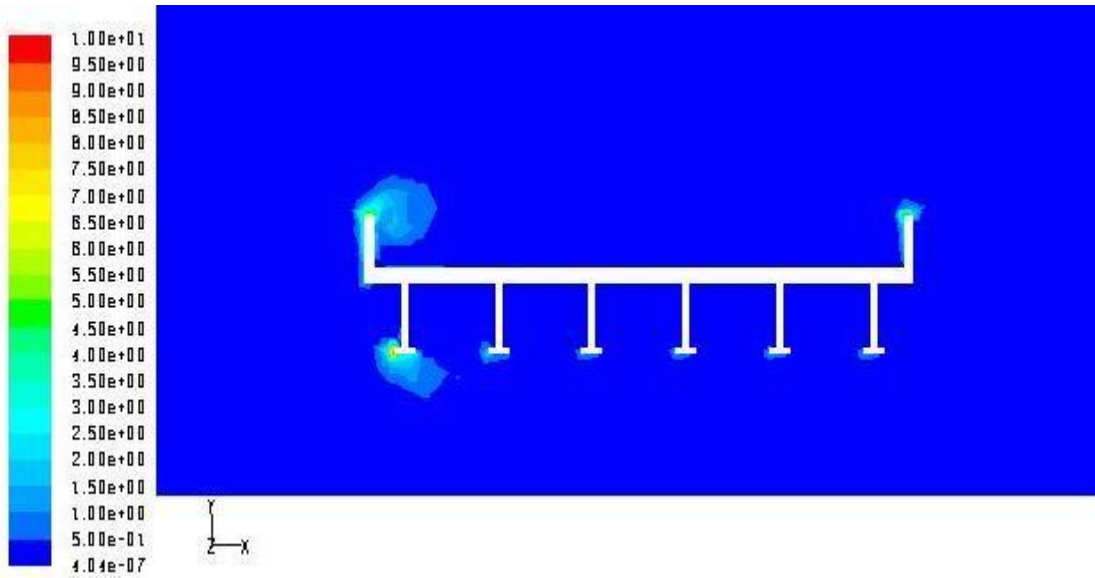


Figure 4.7(a) Contours of Turbulence Dissipation around the Bridge Deck for the Prototype

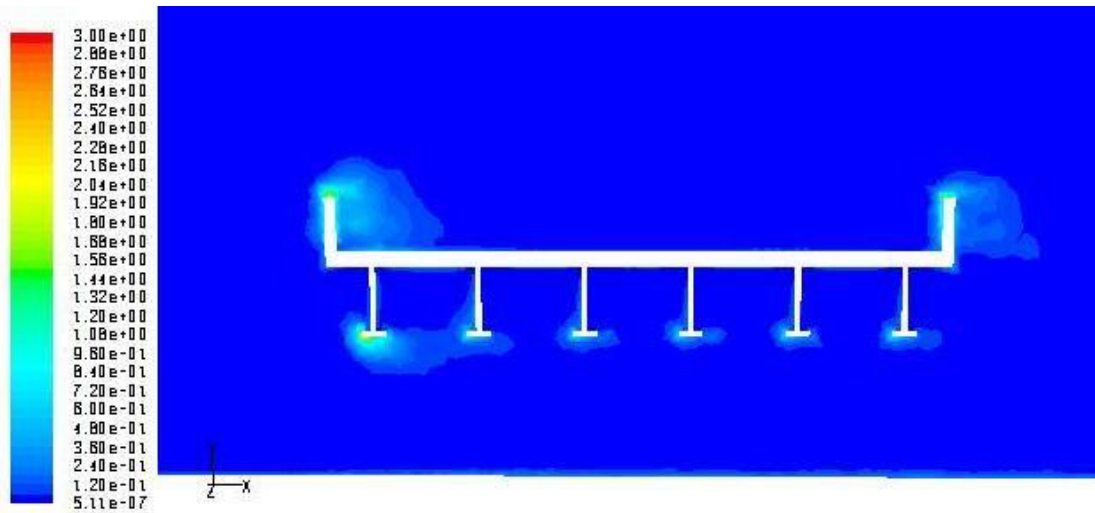


Figure 4.7(b) Contours of Turbulence Dissipation around the 1.5:1 Scaled Bridge Deck

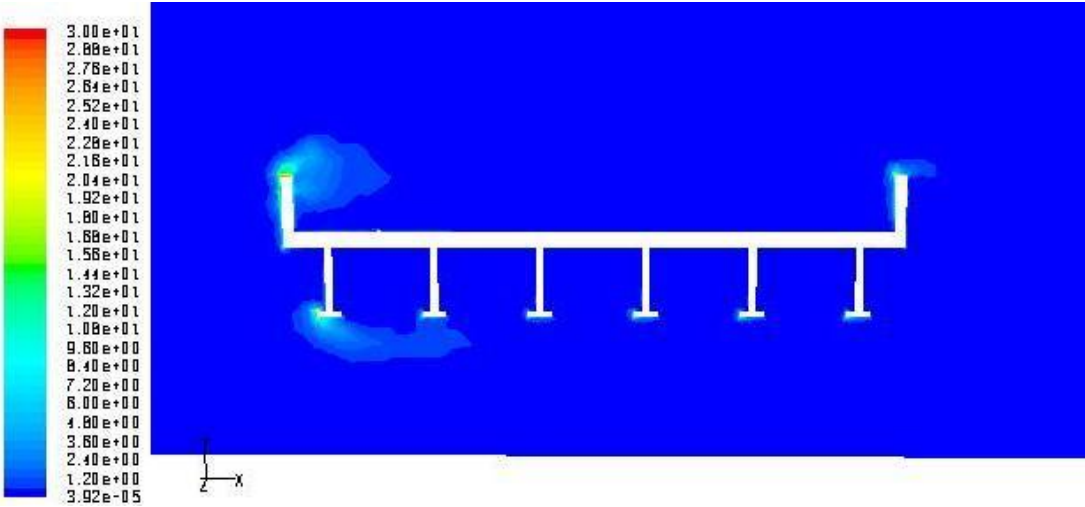


Figure 4.7(c) Contours of Turbulence Dissipation around the 1:3.1 Scaled Bridge Deck

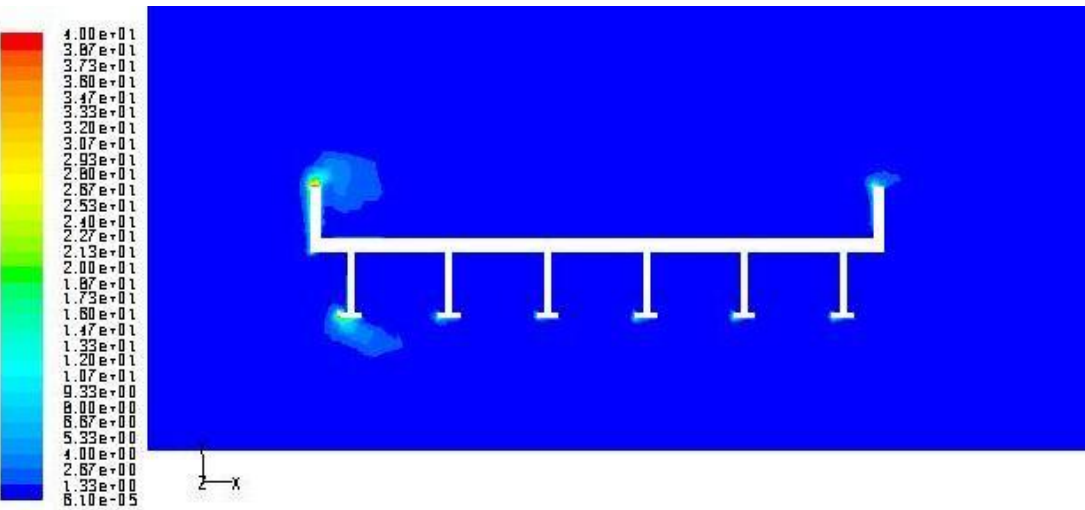


Figure 4.7(d) Contours of Turbulence Dissipation around the 1:5.1 Scaled Bridge Deck

4.2.5 Shear Stress distribution

Shear stress is the force applied by a flowing liquid to its boundary. When an object is immersed in a moving fluid the interaction will occur between the body and the fluid surrounding it, which produces the forces at the fluid-body interface. The forces acting *normal* to the free stream direction are wall shear stresses. Due to the influence of viscosity and the forces

acting parallel to the free-stream direction may be called normal stresses pressure. The resultant force of stress and pressure distribution in the direction of flow is the drag force. Figures 4.8 (a) to 4.8 (d) illustrate the distribution of the shear stress on the bridge deck. The uneven distribution of the shear stress on bridges where shear stresses are higher at the front of the bridge deck shown with red region and lower shear stress at the rear end of bridge shown with blue color. The uneven distribution of the stresses can lead to instability of the bridge. As expected, the magnitude of shear stress for 5:1 scaled model was found to be 10 times higher than the 1.5:1 scaled model. In terms of the overall distribution of shear stress on the surface of the scaled bridge deck, the model looked similar to the prototype.

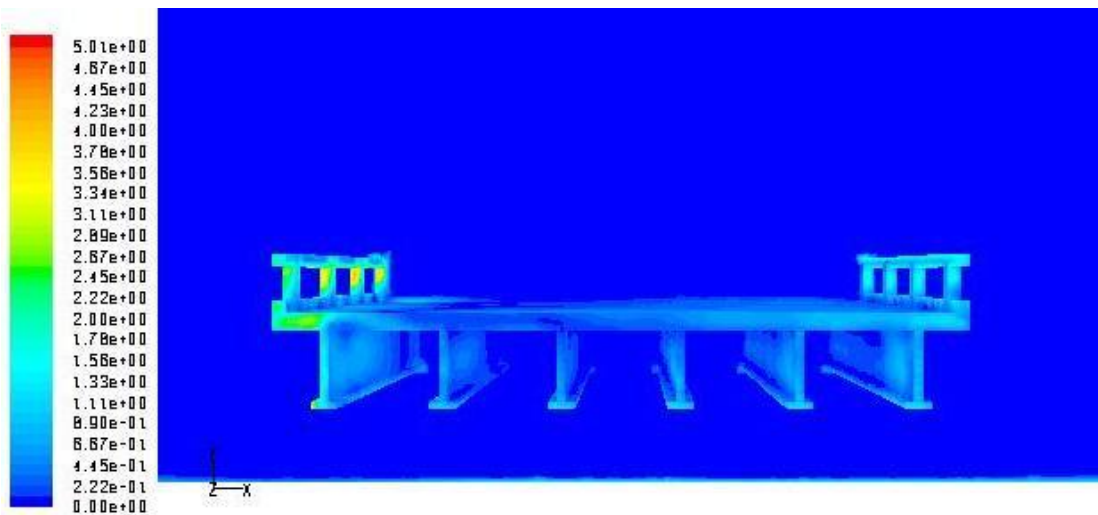


Figure 4.8(a) Contours of Shear Stress on the Bridge Deck for Prototype

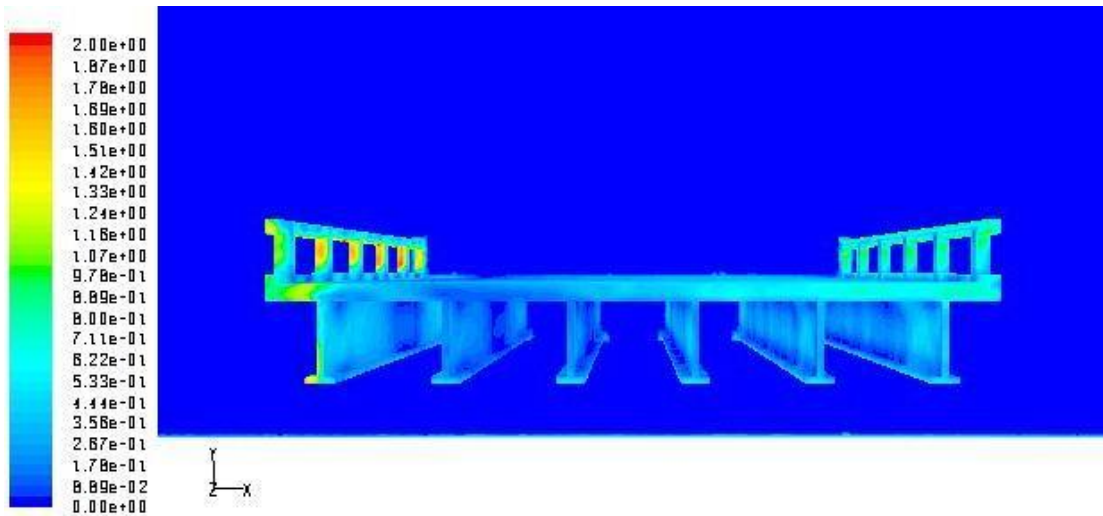


Figure 4.8(b) Contours of Shear Stress on the Bridge Deck for 1.5:1 Scaled Bridge Deck

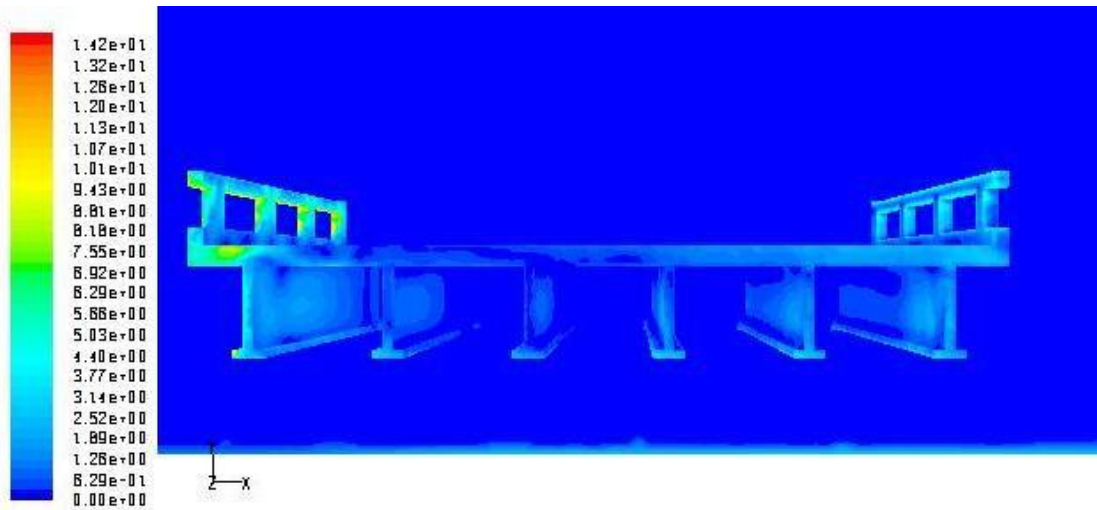


Figure 4.8(c) Contours of Shear Stress on the Bridge Deck for 1:3 Scaled Bridge Deck

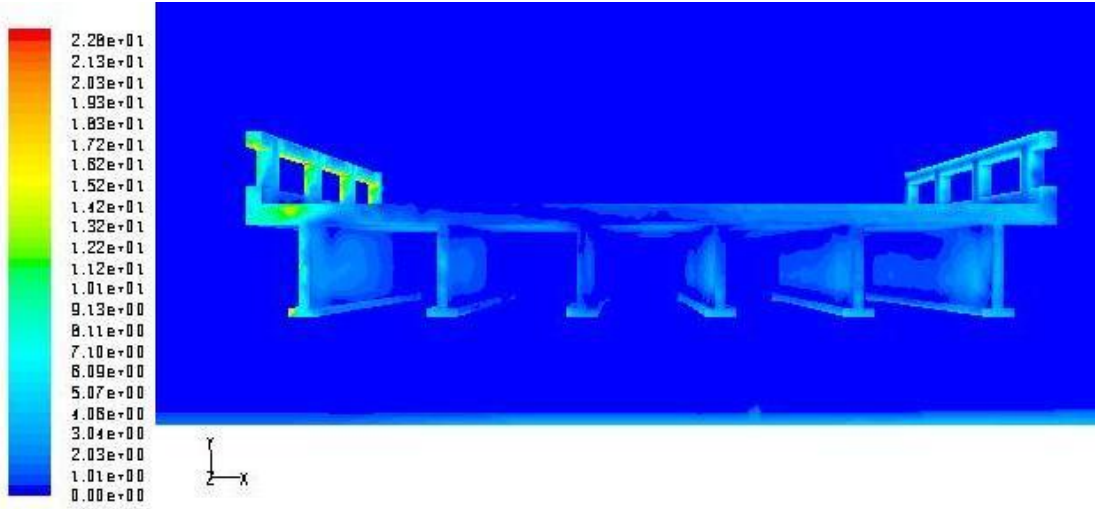


Figure 4.8(d) Contours of Shear Stress on the Bridge Deck for 1:5 Scaled Bridge Deck

Chapter 5 Conclusions

In the present CFD study, six-girder bridge deck models (1:1) were initially validated with the experimental data. The methodology was then used to predict the effect of scaling by using a six-girder bridge deck model scaled to a factor of 1:1.5, 1:1, 3:1 and 5:1. The computed values of drag, lift and moment coefficient for the scaled bridge deck were compared with the simulation results obtained from the experiments for a 1:1 scaled bridge deck. After validating the CFD results (for 1:1 scaled bridge deck model) with the experiments, a small sized bridge deck, 1:1.5, was simulated and the results were compared. Later large sized bridge decks, 3:1 and 5:1, were used to analyze the effect of scaling. The drag coefficient for large and small sized bridges did not show any effect of scaling. The drag coefficient at a higher inundation ratio for a scaled bridge deck model and prototype was found to be approximately 2.2. The lift coefficient showed an overall difference of around 15% in the large and small size bridge decks. This may be due to the difficulties in meeting both Froude number similarity and Reynolds number similarity, since the Reynolds number similarity was neglected. The moment coefficient did not show any effect of scale for the complete range of inundation ratio; therefore, ignoring the Reynolds number similarity in the modeling approach did not show any significant effect on the non-dimensional moment coefficient and drag coefficient. A further detailed study for the practical design scale bridge, or 40:1, could not be done because of the significant computational time required for realistic bridges.

References

1. Afzal, N., A. Bushra, and Abu Seena. "Power law velocity profile in transitional rough pipes." *Journal of fluid Engineering, Trans ASME* 128 (2006): 548-558.
2. Afzal, N., A. Bushra, and Abu Seena. "Power law velocity profile in transitional rough pipes." *Journal of fluid Engineering, Trans ASME* 128 (2006): 548-558.
3. Afzal, N., and A. Bushra. "Structure of the turbulent hydraulic jump in a trapezoidal channel." *Journal of hydraulic Research IAHR* 40.2 (2002): 205-214.
4. Seena A., A. Bushra, and N. Afzal. "Logarithmic expansions for Reynolds shear stress and Reynolds heat flux in a turbulent channel flow." *J. HEAT TRANSFER, Trans. ASME* 130 (2008): 1-4.
5. Denson, K. H. "Steady-state drag, lift, and rolling-moment coefficients for inundated inland bridges." Rep. No. MSHD-RD-82-077. Springfield, VA: Reproduced by National Technical Information Service, 1982.
6. Douglass, S. L., Q. J. Chen, J. M. Olsen, B. L. Edge, and D. Brown. "Wave forces on bridge decks." *Draft Report for FHWA*. Washington, DC: U.S. Dept. Transp., Fed. Hwy. Administration, 2006
7. "FLUENT 6.3 Help Documentation." Fluent Inc.
8. Guo, J. "Hunter Rouse and Shields Diagram." Proc. 13th IAHR-APD Congress. *World Scientific* 2 (2002): 1096-1098.
9. Guo, J., and P. Y. Julien. "Modified log-wake law for turbulent flow in smooth pipes." *Journal of Hydraulic Research, IAHR* 41.5 (2005): 493-501.
10. Harlow, F. H., and J. E. Welch. "Numerical calculation of time dependent viscous incompressible flow of fluid with free surface." *The Physics of Fluids* 8.12 (1965).

11. Huang J., Y. G. Lai, and V. C. Patel. "Verification and validation of 3-D numerical model for open channel flows." *Numerical Heat Transfer Part B* 40 (2001): 431-439.
12. Kerényi, K., T. Sofu, and J. Guo. "Modeling hydrodynamic forces on bridge decks using supercomputer." *Public Roads* 72.2 (2008).
13. Koshiznka, S., H. Tamako, and Y. Oka. "A particle method for incompressible viscous flow with fluid fragmentation." *Computational Fluids Dynamics* 4 (1995): 29-46.
14. Liaw, K. F. "Simulation of flow around bluff bodies and bridge deck sections using CFD." PhD Diss., University of Nottingham, 2005.
15. Malavasi, S., and A. Guadagnini. "Hydrodynamic loading on river bridges." *Journal of Hydraulic Engineering* 129.11 (2003): 854-861.
16. Maronnier V., M. Picasso, and J. Rappaz. "Numerical simulation of free surface flows." *Journal of Computational Physics* ISS (1999): 439-455.
17. Matsuda, K., K. R. Cooper, H. Tanaka, M. Tokushige, and T. Iwasaki. "An investigation of Reynolds number effects on the steady and unsteady aerodynamic forces on a 1:10 scale bridge deck section model." *Journal of Wind Engineering and Industrial Aerodynamics* 89 (2001): 619-632.
18. Mohapatra P. K., S. Bhallamudi, and V. Eswaran. "Numerical study of flows with multiple free surfaces." *International Journal of Numerical Methods in Fluids* 36 (2001): 165-184.
19. Naudascher, E., and H. J. Medlarz. "Hydrodynamic loading and backwater effect of partially submerged bridges." *Journal of Hydraulic Research* 21.3 (1983): 213-232.
20. Okajima, A., D. Yi, A. Sakuda and T. Nakano. "Numerical study of blockage effects on aerodynamic characteristics of an oscillating rectangular cylinder." *Journal of Wind Engineering and Industrial Aerodynamics* 67-68 (April-June 1997): 91-102.

21. Ramamurthy A. S., Junying Qu, and Oiep Vo. "Volume of fluid model for open channel flow problem." *Canadian Journal of Civil Engineering* 32.5 (2005): 996-1001.
22. Ramamurthy A. S., Junying Qu, and Oiep Vo. "VOF model for simulation of a free overfall in trapezoidal channel." *Journal of Irrigation and Drainage Engineering* 132.4 (2006): 425-428.
23. Tainsh, J. "Investigation of forces on submerged bridge beams." Rep. No. 108. Dept. of Public Works. Sydney, Australia: New South Wales U, 1965.
24. Ye, J., and J. A. McCorquodale. "Simulation of curved open channel flows by 3D hydrodynamic model." *Journal of Hydraulic Engineering* 124.7 (1998): 687- 698.
25. Young, D. F., B. R. Munson, and T. H. Okiishi. *A brief introduction to fluid mechanics*. 3rd Edition. 2004.
26. Zhaoding, X., A. Bushra, S. Tanju, K. Kornel, and J. Guo. "CFD Modeling of drag and lift of inundated bridge decks." 33rd IAHR Congress held from August 10-14, 2009. Water Engineering for Sustainable Environment, Vancouver, Canada, 2009.
27. [http://www.cfd-online.com/Wiki/Two equation turbulence models](http://www.cfd-online.com/Wiki/Two%20equation%20turbulence%20models)
28. [http://www.cfd-online.com/Wiki/RNG k-epsilon model](http://www.cfd-online.com/Wiki/RNG%20k-epsilon%20model)

Appendix A. Experimental Data

h_b [m]	h^*	$Fr = 0.16$			$Fr = 0.22$		
		C_D	C_L	C_M	C_D	C_L	C_M
0.23	0.34	1.20	-0.07	0.08	1.30	-0.10	0.10
0.22	0.52	1.24	-0.01	0.09	1.28	-0.04	0.03
0.21	0.69	0.83	-1.02	0.26	0.49	-1.70	0.30
0.20	0.86	0.80	-1.21	0.24	0.81	-1.20	0.24
0.19	1.03	0.84	-1.56	0.30	0.86	-1.51	0.27
0.18	1.21	1.09	-1.21	0.23	1.08	-1.30	0.23
0.17	1.38	1.30	-1.00	0.19	1.30	-1.08	0.19
0.16	1.55	1.54	-0.65	0.13	1.55	-0.76	0.12
0.15	1.72	1.62	-0.49	0.09	1.63	-0.59	0.09
0.14	1.90	1.65	-0.40	0.07	1.72	-0.46	0.06
0.13	2.07	1.74	-0.33	0.06	1.79	-0.37	0.04
0.12	2.24	1.72	-0.26	0.06	1.78	-0.30	0.04
0.11	2.41	1.77	-0.22	0.05	1.82	-0.23	0.02
0.10	2.59	1.79	-0.17	0.04	1.84	-0.18	0.02
0.09	2.76	1.80	-0.12	0.04	1.87	-0.14	0.01
0.08	2.93	1.80	-0.06	0.03	1.91	-0.10	0.00
0.07	3.10	1.81	-0.03	0.03	1.94	-0.05	0.00
0.06	3.28	1.81	0.01	0.02	1.94	0.00	-0.02

h_b [m]	h^*	Fr = 0.28			Fr = 0.32		
		C_D	C_L	C_M	C_D	C_L	C_M
0.23	0.34	1.65	-0.06	0.06	1.85	-0.06	0.03
0.22	0.52	1.44	-0.06	0.02	1.45	-0.36	0.03
0.21	0.69	0.95	-1.33	0.17	1.10	-1.07	0.10
0.20	0.86	1.13	-0.88	0.11	1.16	-0.95	0.09
0.19	1.03	1.07	-1.16	0.15	1.21	-1.01	0.09
0.18	1.21	1.23	-1.02	0.13	1.36	-0.86	0.06
0.17	1.38	1.43	-0.84	0.09	1.59	-0.74	0.02
0.16	1.55	1.71	-0.58	0.03	1.85	-0.49	-0.02
0.15	1.72	1.82	-0.42	0.01	1.99	-0.40	-0.04
0.14	1.90	1.84	-0.34	0.01	2.07	-0.28	-0.06
0.13	2.07	1.91	-0.30	0.00	2.18	-0.20	-0.06
0.12	2.24	1.94	-0.25	-0.02	2.15	-0.19	-0.07
0.11	2.41	1.92	-0.24	-0.01	2.12	-0.20	-0.08
0.10	2.59	1.91	-0.18	-0.02	2.11	-0.21	-0.07
0.09	2.76	1.98	-0.15	-0.02	2.11	-0.22	-0.06
0.08	2.93	1.99	-0.12	-0.02	2.11	-0.19	-0.07
0.07	3.10	2.01	-0.08	-0.02	2.11	-0.14	-0.07
0.06	3.28	2.02	-0.04	-0.03	2.11	-0.10	-0.07